2016

# Phenanthrene...With a Twist!

Nicholas S. Kim
*Colby College*

# Phenanthrene…With a Twist!

By Nicholas S. Kim

A Thesis Presented to the Department of Chemistry,
Colby College, Waterville, ME
In Partial Fulfillment of the Requirements for Graduation With Honors
in Chemistry

Submitted May 16, 2016

# Phenanthrene…With a Twist!

By Nicholas S. Kim

**Approved:**

_____
Dasan M. Thamattoor, Ph.D., Mentor
Professor of Chemistry

_____ Date

_____
Nicholas Boekelheide, Ph.D., Reader
Assistant Professor of Chemistry

_____ Date

# Vitae

Nicholas Seung Min Kim was born September 19, 1994 to Jemma E. Kim and Jason M. Kim in Los Angeles, CA. He grew up in Claremont, CA where he attended Chaparral Elementary and El Roble Middle School. In 2008, he moved to Diamond Bar, CA where he attended Walnut High School and discovered his interest in chemistry.

In 2012, he matriculated at Colby College and made the trek to the east coast, seeking novel experiences. His first year, he volunteered at Atwood Primary School in Oakland as a teacher's assistant and played on the club water polo team. Additionally, he joined the NCAA DIII swimming and diving team, forging his way to captainship by his senior year. At the end of his second year, he joined Professor Dasan Thamattoor's organic chemistry research laboratory and began volunteering at Lakewood Continuing Care Center. Starting his junior year, he immersed himself in the Department by accepting tutoring and laboratory teachers' assistant positions in organic chemistry. During JanPlan of 2015, he had the opportunity to shadow Dr. Peverada, a thoracic surgeon at Maine General Hospital and to further a clinical research project.

Academically, Nicholas majored in Chemistry and minored in Studio Art: Sculpture. He took a wide variety of courses outside of his comfort zone including Literature by Women of Color, Statistical Methods of Analysis, Ireland and Otherness: James Joyce, and Sculpture I-IV. Although he did not take any semesters abroad, he travelled to Nairobi, Kenya (Aug 2009) to provide medical relief with International Medical Relief and to Bochum, Germany (June 2015) with Professor Thamattoor and labmate Nate Flanders to conduct research on carbenes at Ruhr Universitat.

In the future, Nicholas plans to pursue a career in medicine.

# Acknowledgements

Without the following people, I would be lost:

My mother and grandmother: Jemma Eunsil Kim and Young Sook Chon, for showing me what it means to be courageous and patient.

Professor Thamattoor, who played a large part in hypnotizing me with his spellbinding lectures to declare a chemistry major. Also, I want to thank him for bestowing upon us all three daily remedies: mirthful laughter, witty jokes, and eloquent anecdotes.

The Colby community: friends, teammates, faculty, and staff for helping make Mayflower Hill a challenging, inspiring, and inclusive space—a place where I can experiment, take risks, fail, and ultimately discover the latent beauty in things.

# Contents

# Figures & Tables

**Introduction**

# Figures & Tables (Continued)

**Results and Discussion**

# Abstract

The twisted and sterically hindered 4,5-dibromophenanthrene, was synthesized from 2,6-dibromoiodobenzene in a four-step pathway, or from 1,3-dibromobenzene in a three-step pathway. Then, 4,5-dibromophenanthrene was subjected to a Kumada coupling, leading to the synthesis of an even more twisted 4-bromo-5-*tert*-butylphenanthrene. Computational studies using density functional theory were performed to compare experimental and theoretical characteristics of these compounds, such as dihedral angles, optimized structures, and transition state energy barriers.

The purpose of these experiments is to fill gaps in chemical databases, synthesize more pronounced twists in normally planar phenanthrene molecules, and to ultimately synthesize 4,5-bis-*tert*-butylphenanthrene, which may have interesting spectral results due to the close proximity of its substituent *tert*-butyl groups.

# Introduction

*Overview*

Phenanthrene molecules belong to a larger category of compounds called polycyclic aromatic hydrocarbons or PAHs. Specifically, phenanthrene (Figure 1) is a structural isomer of anthracene, which is a linear arrangement of three benzene rings. Additionally, phenanthrenes, and many simple PAHs are planar molecules.

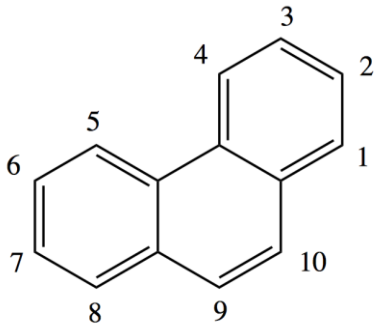


**Figure 1.** Phenanthrene and numbering of positions.

Phenanthrenes play a unique and crucial role in chemistry. In the medical field, phenanthrene, along with other PAHs like benzo[a]pyrene, is a known constituent of cigarette smoke and has been found—when smoked—to be converted into diol epoxides, which are highly carcinogenic.[2] The slightly twisted nature of the diol epoxides may expose the reactive epoxide site, leading to an increase in reactivity. In a different light, phenanthrenes form the core structure of opiates such as morphine and codeine, as shown in Figure 2. The twisted nature of these opiates may provide direction and specificity for the interaction with μ-opioid binding sites located in the brain.

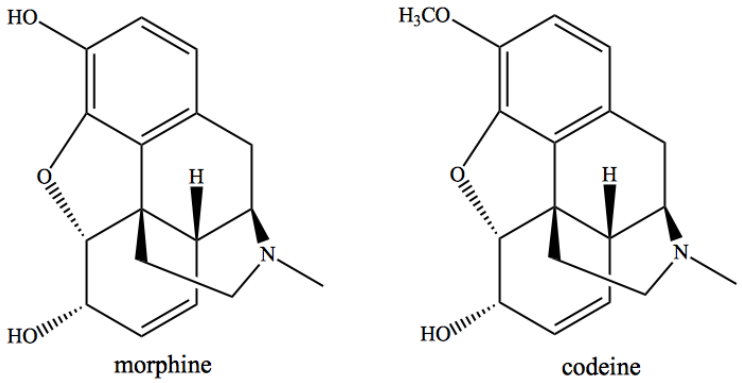


**Figure 2.** Chemical structures of morphine and codeine.

Due its aromaticity, phenanthrene is planar. However, when substituents are added to the 4 and 5 positions (called the bay area), the molecule starts to twist away from planarity due to the steric interactions between substituent groups as shown in Figure 3.

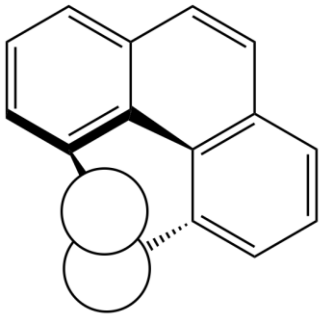

**Figure 3.** Representation of a twisted phenanthrene

Phenanthrenes are also recurring compounds in Professor Thamattoor's lab, where other investigators synthesize phenanthrene-based precursors for the photochemical generation of carbenes as shown in Figure 4.

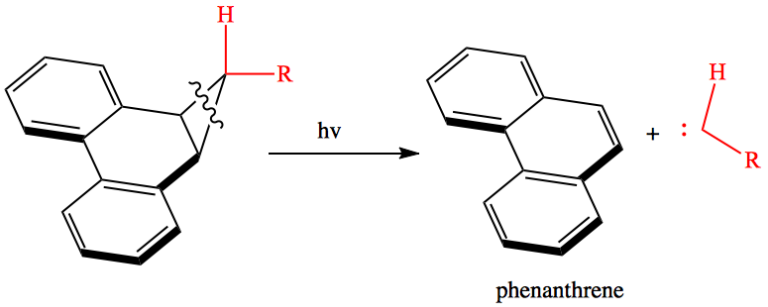


**Figure 4.** Photochemical generation of carbenes from phenanthrene-based precursor

*Generation of Twisted Phenanthrenes*

A common method of generating twisted phenanthrene is from the photochemical cyclization of a stilbene in the presence of oxygen and a catalytic dose of iodine, as shown by Frank Mallory.[3] Irradiation with light renders the cis/trans stereochemistry of the stilbene irrelevant, due to photochemical conversion of the trans isomer into the cis form.

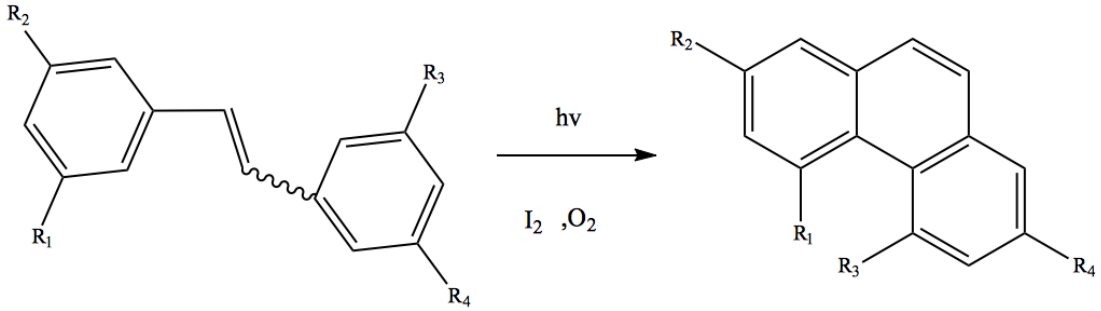


**Figure 5.** The Mallory reaction for photochemically generating phenanthrenes

In addition to Mallory's reaction, shown in Figure 5, it has been shown that other, more extensive polycyclic aromatic hydrocarbons can be synthesized. For example, Thomas Katz et al. showed that helicenes can be synthesized through a photochemical procedure similar to the Mallory method. In 1991, he modified Mallory's recipe to increase the synthesis yields of the polycyclic aromatic hydrocarbons and to decrease the

generation of side products. As shown in Figure 6, Katz reported using two equivalents of iodine, excess propylene oxide, and an inert atmosphere was more effective in generating twisted phenanthrenes.[4] In addition, Katz showed that other substituents—in his case, bromine—could influence stereochemistry of the photocyclization product.[5]

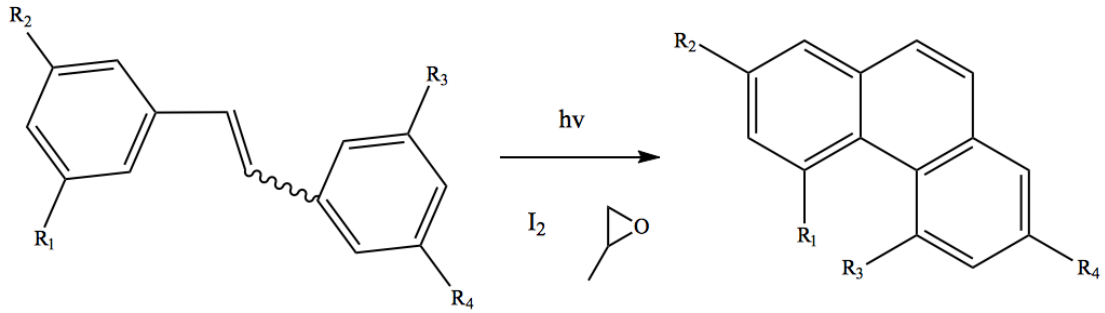


**Figure 6.** The Katz reaction for photochemically generating phenanthrenes

More recently, in 2012, Wang et al. determined another method for the generation of polycyclic aromatic compounds using heat. As shown in Figure 3 below, dicarbonyl compounds can be converted into their corresponding bis(N-tosylhydrazone)s by reaction with p-toluenesulfonyl hydrazide. The resulting compound can then be converted into its corresponding phenanthrene through a carbene intermediate in the presence of three equivalents of LiO*t*Bu, a catalytic amount of rhodium, and heat. [6]

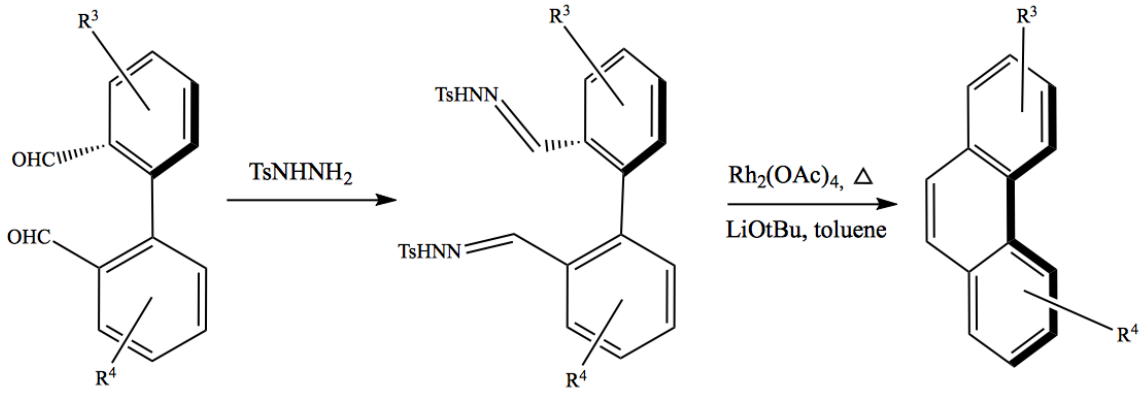


**Figure 7.** The Wang reaction for thermochemically generating phenanthrenes

Like the previous methods, this approach maintains the flexibility in the choice of substituent groups. In contrast, it provides an alternative method to those involving photochemical techniques. The Wang method was preferred for use in experiments due to the availability of reagents and the higher degree of success obtained with the available apparatuses.

*Previous Works*

In the past, a variety of polycyclic aromatic compounds, such as helicenes, have been synthesized. Helicenes are complex PAHs—which resemble extensions of phenanthrenes—arranged in an angular fashion to form a helical shape. Carbohelicenes have been synthesized through a variety of methods, including photocyclizations, Diels-Alder reactions, Friedel Crafts-type reactions, metal-catalyzed cyclizations, and radical cyclizations. In 1967, Martin et al. reported the first synthesis of heptahelicene **(A)** via photochemical methods.[6b] Another relevant example is the synthesis of a helicenes **(B)** using a radical double-cyclization approach, reported by Wang et al.[6c]

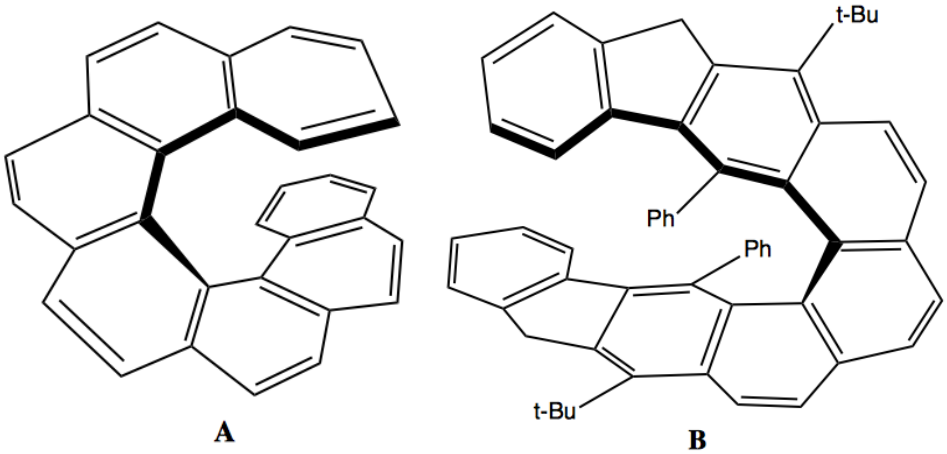


**Figure 8.** Previously synthesized helicenes

Twisted phenanthrenes have also been synthesized in the past. For example, Mannschreck et al. managed to synthesize a methyl-*tert*-butyl phenanthrene (Figure 9) in 1983 through a photochemical procedure similar to that used by the Mallory group.[7]

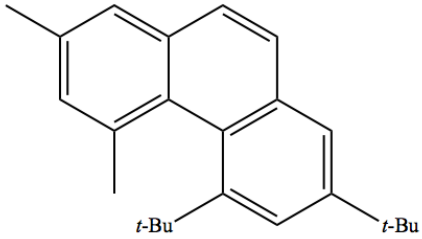


**Figure 9.** 2,4-dimethyl-5,7-bis-*tert*-butylphenanthrene

In 2013, James Shaum from Colby College synthesized 2,4-dimethyl-5,7-diphenylphenanthrene (Figure 10) also using the Mallory reaction template.[8]

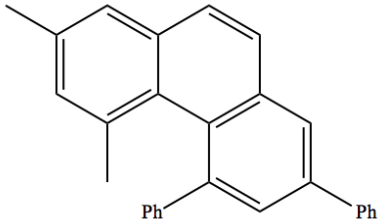


**Figure 10.** 2,4-dimethyl-5,7-diphenylphenanthrene

Shaum discovered that the degree of twist in the above phenanthrene was 30.3°. By extension, it is expected that larger groups in the bay area would take up more volume, inducing a larger degree of twist in the phenanthrene backbone.

*Phenanthrene Characterization*

One can quite easily determine the angle of twist by measuring the dihedral angle about the bay area, as shown below in the phenanthrene scheme. The dihedral angles of the bonds between the starred carbon atoms in Figure 11 can be a standard for measuring the twisted nature of a given phenanthrene molecule.

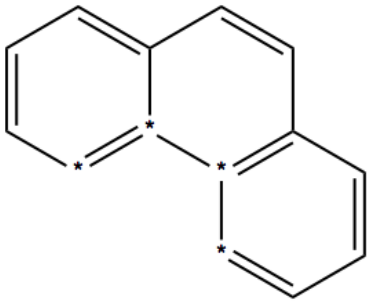

**Figure 11.** Measurement of twist in phenanthrene via dihedral angles between starred carbons.

Due to the chirality of twisted phenanthrenes, it is also possible to calculate the energy barrier for the enantiomeric interconversion (Figure 12).

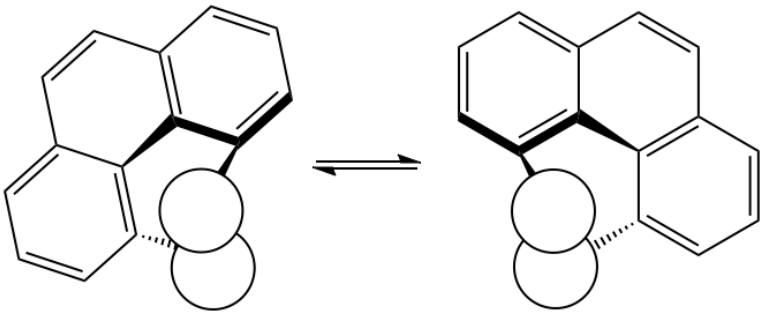

**Figure 12.** Enantiomeric interconversion of twisted phenanthrenes

*Project Goals*

In my project, I undertook the synthesis of 4,5-dibromophenanthrene and 4,5-bis-*tert*-butylphenanthrene (Figure 13, **4** and **5**, respectively) from their corresponding dialdehyde compounds using the thermal method used by Wang's group. The purpose was to subject the phenanthrene compound to as much strain as possible while maintaining its p-orbital overlap for aromaticity.

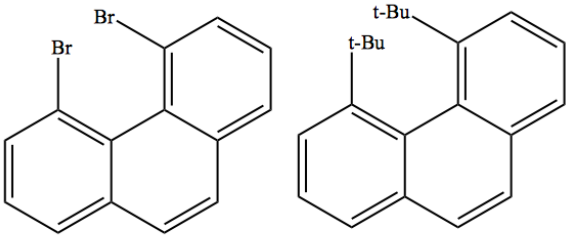


**4** **5**

**Figure 13.** 4,5-dibromophenanthrene (**4**) and 4,5-bis-tert-butylphenanthrene (**5**)

Previous work on 4,5-dibromophenanthrene has been very limited and was only referenced in one paper, which offered no synthesis methods or characterization of the compound whatsoever.[11] Therefore, synthesizing 4,5-dibromophenanthrene would add a novel compound to the chemical database.

In addition, 4,5-bis-*tert*-butylphenanthrene is intriguing as the bis-*tert*-butyl groups in such close proximity of each other could potentially create a molecular gear, thereby restricting free rotation of each group. This obstructive interaction in the bay area would lead to nondegenerate $^{1}$H NMR shifts for each methyl group in the *tert* butyl groups, which normally have degenerate methyl signals.

*Synthetic Plan*

To synthesize 4,5-dibromophenanthrene (**1**), the Wang procedure was followed for the most part other than the use of KO*t*Bu in lieu of LiO*t*Bu, as shown in Figure 14.

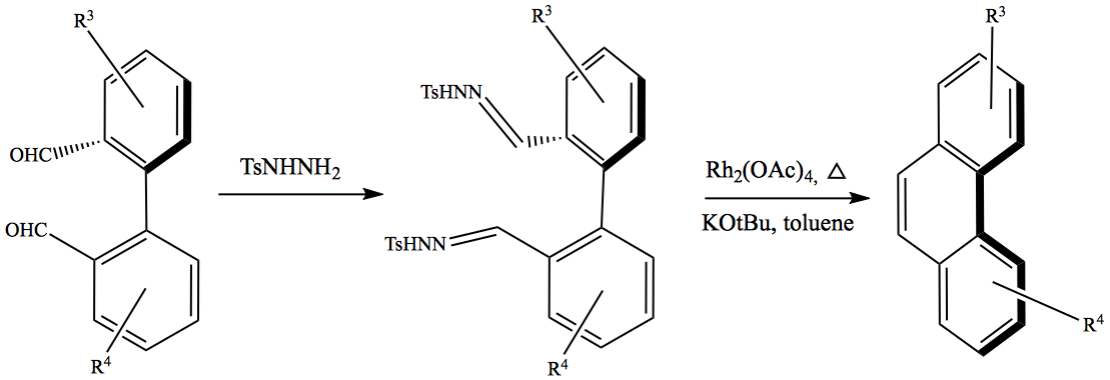


**Figure 14.** Synthesis of 4,5-dibromophenanthrene

Making 4,5-bis-*tert*-butylphenanthrene is slightly more complicated. In 2011, Biscoe et al. used a Kumada coupling procedure to react aryl bromides with *tert*-butyl magnesium halides to form *tert*-butyl aromatic compounds as shown in the scheme below.[9]

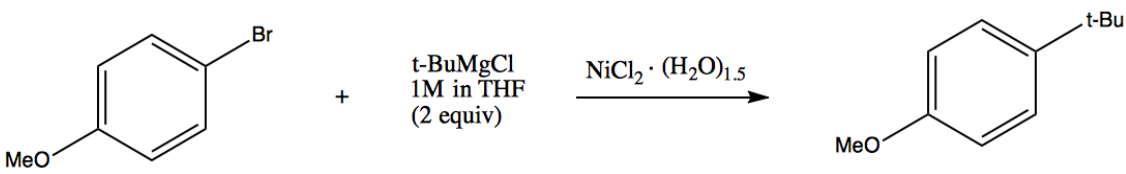


**Figure 15.** Exchange of a halide with a tertiary alkyl group—Biscoe et al.

Using the above process, 4,5-dibromophenanthrene can be converted into 4,5-bis-*tert*-butylphenanthrene using the procedure from Biscoe's group (Figure 16).

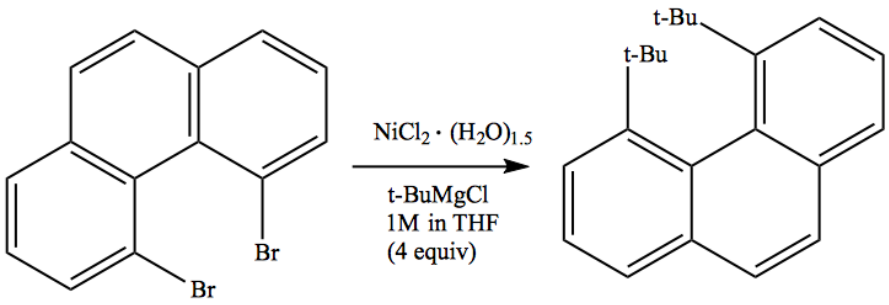


**Figure 16.** Synthesis of 4,5-bis-*tert*-butylphenanthrene using the Biscoe et al. procedure.

*Characterization Plan*

Following the synthesis of 4,5-dibromophenanthrene and 4,5-bis-*tert*-butylphenanthrene, these compounds were isolated and identified using a multitude of spectroscopy tools. Then, single crystals were grown, and X-ray crystallography was used to measure physical traits of these compounds such as: the degree of ring twist in the phenanthrene. Lastly, computational analysis was performed to compare theoretical models of phenanthrenes to the experimental results. To paint a more detailed picture of these compounds, optimization and frequency calculations, and dihedral angle and transition states measurements were conducted using the DFT B3LYP/6-31G (d) method and basis set combination.[14]

Working with twisted phenanthrenes can be fascinating and possibly daunting due to the unlimited number of substituents one can add to the 4,5 position (bay area). Synthesis of the above compounds offers physical insight into twisted phenanthrenes and opens doors to other syntheses in the future.

## Results & Discussion

*Synthesis Results*

To synthesize the two phenanthrene-based products (Figure 12), two different pathways were used: Method 1 and Method 2 (Figure 17).

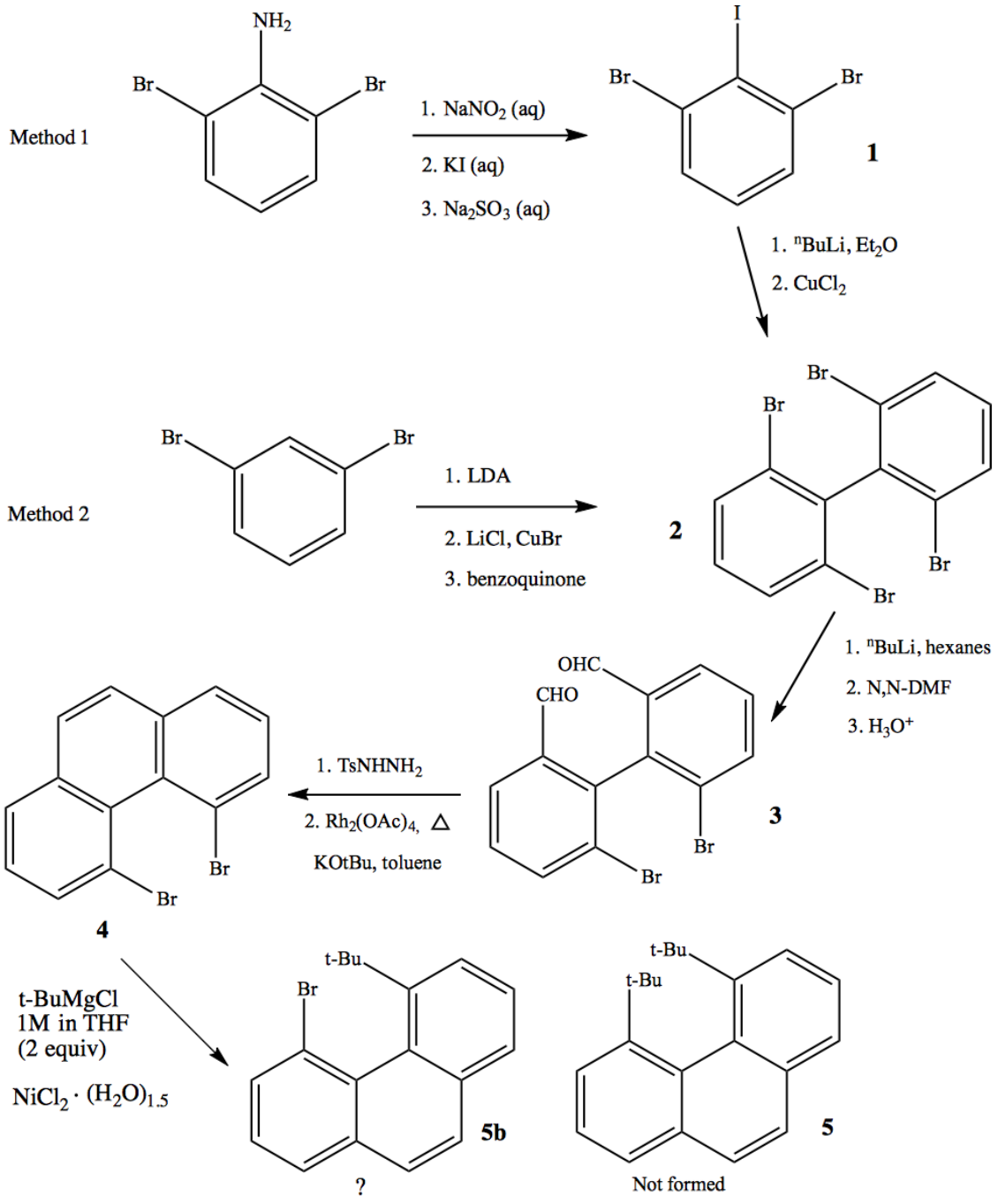


**Figure 17.** Complete Synthesis Pathway

The first method begins with a two-step reaction of commercially available 2,6-dibromoaniline into 2,6-dibromoiodobenzene (**1)** via a Sandmeyer-like reaction.[12] The synthesis of **1** was confirmed by GC/MS (m/z = 361.8) and $^{1}$H NMR spectroscopy, which showed a triplet at 7.09, and a doublet at 7.55, which correspond to the two unique protons on the benzene rings. In addition, the $^{13}$C NMR showed 4 shifts between 109.0 and 131.5, which correspond to the 4 unique carbons on the benzene rings.

Then, compound **1** was subjected to an Ullmann-like reaction involving a bromine-lithium exchange to yield 2,2',6,6'-tetrabromo-biphenyl (**2**).[10] The synthesis of **2** was confirmed by were GC/MS (m/z = 469.8) and $^{1}$H NMR spectroscopy, which showed a doublet shift at 7.65 and a triplet at 7.15, which correspond to the two unique protons on the benzene rings. In addition, the $^{13}$C NMR showed 4 shifts between 124.2 and 142.1, which correspond to the 4 unique carbons on the benzene rings.

The second method is a more efficient one-pot procedure adapted from Perron et al. and also involves an Ullmann-like reaction.[10] Commercially available 1,3-dibromobenzene undergoes aromatic deprotonation with the addition of lithium diisopropylamide (LDA). The subsequent copper transmetallation with the addition of CuBr and reductive elimination of Cu with the addition of benzoquinone yields the tetrabromobiphenyl product (**2**). Although this latter method is more difficult to purify, it was used over the former because it produced comparable yields to the first method and also eliminated a whole step. The spectral results matched the results obtained from the first method.

From **2**, the two pathways converge into a two-step route to the synthesis of 4,5-dibromophenanthrene. The next step involves a Bouveault aldehyde synthesis reaction

through the addition of an organolithium reagent and N,N dimethylformamide (DMF), resulting in the dicarbaldehyde compound (**3**).[13] The synthesis of **3** was confirmed by GC/MS (m/z = 367.8) and $^{1}$H NMR spectroscopy, which showed a singlet shift at 9.60 corresponding to proton of the aldehyde group, and a triplet at 7.55, doublet at 7.95, and doublet at 8.05, which correspond to the protons located directly on the benzene rings. In addition, $^{13}$C NMR showed 7 shifts between 125.5 and 189.5, agreeing nicely with the 7 unique carbons of **3**.

From **3**, compound **4** was synthesized through a rhodium(II)-catalyzed reaction that involved the addition of bis(N-tosyl- hydrazone) and KO*t*Bu. As shown by the Wang group, this procedure allows the formation of an intramolecular C=C bond through a carbene radical intermediate.[6] The synthesis of **4** was verified via NMR spectroscopy, which showed 4 multiplets between δ 7.40 and 7.80, which correspond to the 4 unique protons on the phenanthrene rings. Similar to **3**, **4** has 7 unique carbon shifts that correspond to the protons of phenanthrene. GC/MS analysis showed a parent peak at m/z = 335.9, which corresponds to the molar mass of **4**, and fragments at m/z = 255 and 176, which correspond to **4** after it loses a bromine and two bromines, respectively, and the melting point was found to be between 170-171 °C, which is well above the melting point of phenanthrene (101 °C). Lastly, X-ray crystallography was used to find a crystal structure and confirm the synthesis of **4**, as shown in Figure 18.

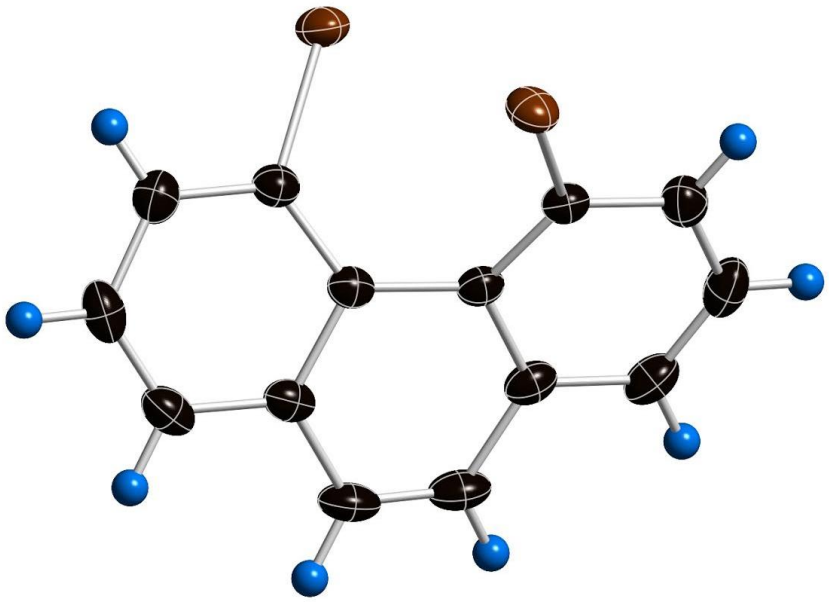

**Figure 18.** X-ray crystal structure of **4**.

From the X-ray data, it was determined that the unit cell of **4** has the following measurements: a = 16.812(3) Å, b = 8.6002(13) Å, and c = 8.1323(12) Å, where a, b, and c correspond to the lengths of the sides of the cell. The angles of the cell are: $\alpha = 90°$, $\beta = 103.745(2)°$, and $\gamma = 90°$. Thus, the crystal was determined to have c-centered monoclinic type cell packing with a volume of 1142.1 $Å^3$ and a refinement value of 2.41%.

From here, the synthesis of 4,5-bis-*tert*-butylphenanthrene was attempted with a Ni-catalyzed Kumada cross-coupling between **4** and a Grignard reagent (1M solution of *t*-butylMgCl). Biscoe et al. discovered through optimization reactions that specifically hydrated $NiCl_2•(H_2O)_{1.5}$ produced the most favorable yields.[8] From GC/MS analysis, it was found that synthesis of 4,5-bis-tert-butylphenanthrene was unsuccessful. However, trace amounts of 4-bromo-5-(*tert*-butyl)phenanthrene were detected via GC/MS (m/z = 312.0 and 314.0), but not isolated.

Figure 19 illustrates the different twisted phenanthrenes synthesized (attempted) in Professor Thamattoor's laboratory. More specifically, the following are the compounds that I have worked with.

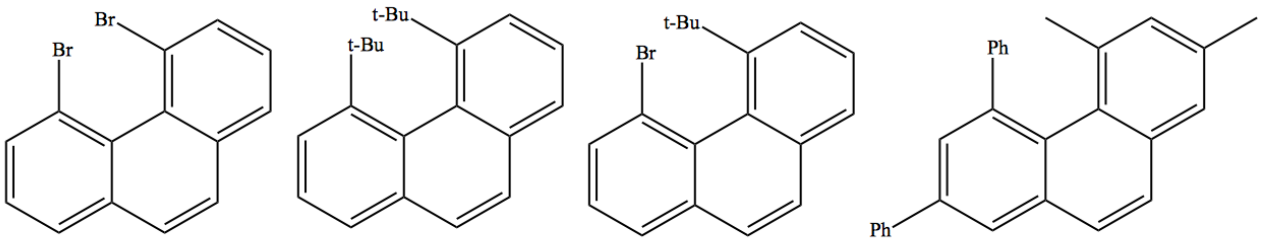


**4** **5** **5b** **6**

**Figure 19.** Comparison of Various Twisted Phenanthrenes

*Computational Results*

All geometry and optimization calculations were performed using Becke's three parameter hybrid density correlation functional of density functional theory (DFT) established by Lee, Yang, and Parr (B3LYP) on Gaussian 09.[15] More specifically, the 6-31G(d) basis set was used for all geometry optimization and frequency calculations. The optimized structures are shown in Figure 20.

Dihedral angles were measured using including C4 and C5 and the in between for**, 4, 5, 5b,** and **6**. These four carbons were chosen because they best represented the twist created by various substituents in each phenanthrene.

Transition state calculations were carried out with QST2 optimizations on the optimized enantiomers of **4, 5, 5b**, and **6** with the B3LYP/6-31G(d) method, but the enantiomeric interconversion was only allowed for **4**. These calculations were followed up with frequency calculations to confirm imaginary normal modes of each transition state.

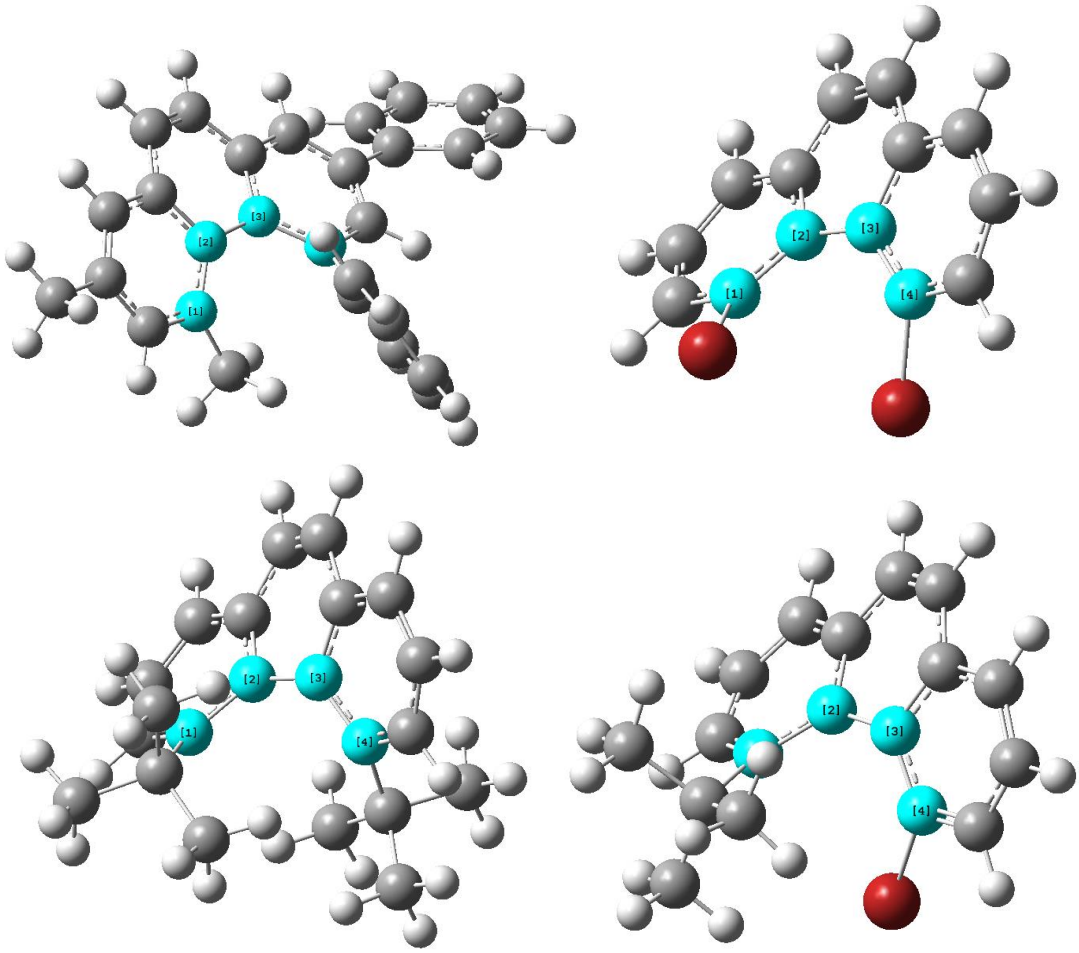

**Figure 20.** Optimized structures of various twisted phenanthrenes. Clockwise from the top left: 2,4-dimethyl-5,7-diphenylphenanthrene, 4,5-dibromophenanthrene, 4-bromo-5-*tert*-butylphenanthrene, and 4,5-bis-*tert*-butylphenanthrene.

The calculated and actual dihedral angles in the bay area of each phenanthrene are listed in Table 1. Also, due to the chiral nature of twisted phenanthrenes, it is possible to calculate the energy barrier for the enantiomeric interconversion of **4** (Table 2, Figure 21).

**Table 1.** Energies, and Calculated and Actual Dihedrals for **4-5b**, and **6**.

| Compound | Calculated Dihedral | Actual Dihedral (°) |
|---|---|---|
| **4** | 34.32 ° | 32.8 ° |
| **5b** | 36.76 ° | n/a |
| **5** | 47.32 ° | n/a |
| **6** [8] | 30.08 ° | 30.31 ° |

**Table 2**. Comparison of Transition State Energy Barriers for **4**

| Compound | ‡ Energy Barriers |
|---|---|
| **4** | 20.3 kcal/mol |

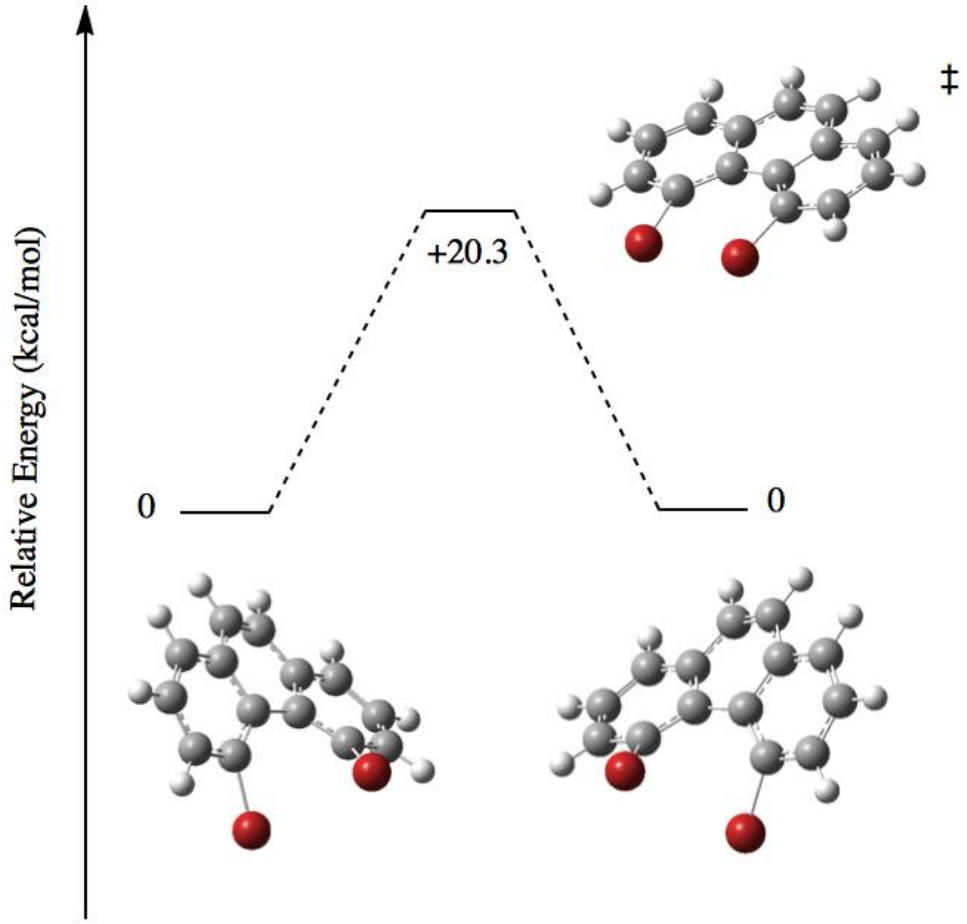


**Figure 21.** Transition State for the Enantiomeric Interconversion of **4**

Unfortunately, the energy barriers for **5**, **5b**, and **6** could not be calculated due to the steric restrictions in the phenanthrene bay area. Interestingly, the energy barrier for 4,5-dibromophenanthrene was not substantial: a slightly higher energy than what is available at room temperature, indicating that the enantiomeric interconversion is not very difficult.

## Conclusion/Future Work/Plot Twists

Under the reaction pathways and conditions of my research, 4,5-dibromophenanthene **(4)** and possibly 4-bromo-5-*tert*-butylphenanthrene **(5b)** were synthesized. However, it was determined that the reaction conditions were not optimal for the synthesis and isolation of 4,5-bis-*tert*-butylphenanthrene **(5)**.

Future syntheses pathways for **5** may include one that performs the Kumada coupling with **3** before the rhodium(II)-catalyzed intramolecular C=C bond formation in hopes that the smaller steric hindrance in **3** would allow for easier cross coupling with the *tert*-butyl Grignard reagent. Another hope for the future is that other substituents, such as adamantane and triptycene, may be added to the bay area of the phenanthrene to induce a much larger twist and energy barrier for enantiomeric interconversion.

# Experimental

*General Procedures*

All manipulations were conducted at ambient pressure unless noted otherwise. Tetrahydrofuran and diethyl ether was dried by passage through two columns (2 ft x 4 in) of activated alumina. All solvents and reagents were used as obtained from commercial sources. The synthesis of 1,3-dibromo-2-iodobenzene **(1)** and 4,5-dibromophenanthrene **(4)** were carried out following literature procedures.[12, 6] All other reactions were carried out under an argon atmosphere in oven dried glassware. Flash chromatography was performed using a Teledyne ISCO Combiflash Rf 200 instrument on pre-packed silica gel columns (70-230 mesh). NMR spectra were recorded at 500 MHz for $^{1}H$ and 125 MHz for $^{13}C$ in the indicated solvents. NMR spectra were recorded at 500 MHz for $^{1}H$ and 125 MHz for $^{13}C$ in $CDCl_3$. The shifts are reported in δ ppm and referenced to tetramethylsilane (TMS). Infrared spectra were recorded on a Perkin-Elmer Spectrum One FT-IR Spectrometer and analyzed with OPUS software. Melting point data were recorded with the OptiMelt Automated Melting Point System. GC/MS data were obtained with a capillary gas chromatograph interfaced with a quadrupole, triple-axis mass selective detector operating in the electron impact (EI) mode.

*Synthesis Methods*

1,3-dibromo-2-iodobenzene **(1)**. [12]

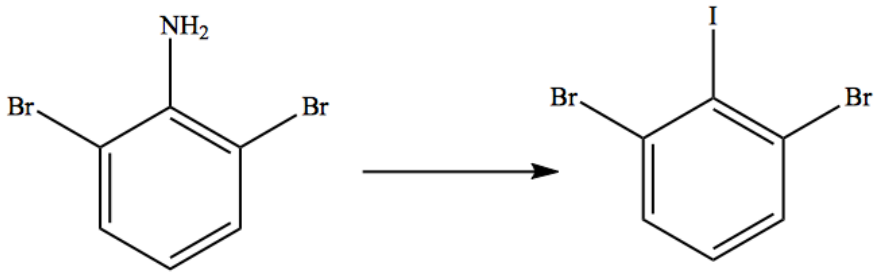


To a milky white suspension of 2,6-dibromoaniline (13.1 g, 52.5 mmol) in 12 M HCl (50 mL) at 0 ºC, a solution of $NaNO_2$ (4.0 g, 58 mmol) in $H_2O$ (30 mL) was added drop wise producing an orange color and heat. Then, this mixture was stirred for 2 hrs. Another batch of $NaNO_2$ (1.0 g, 15 mmol) in 20 mL of $H_2O$ was added to the mixture and stirred for 45 min. Then, over 15 min, this yellow-orange reaction mixture was slowly added to a solution of KI (86.1 g, 519 mmol) in $H_2O$ (130 mL), at 0 ºC producing a foamy maroon solution. The solution was warmed to room temperature and stirred for 16 h and 30 min, yielding a black solution. To this mixture, a solution of $Na_2SO_3$ (7.1 g, 57 mmol) in $H_2O$ (55 mL) was added, producing a clear yellow mixture. The addition of 100 mL of $CH_2Cl_2$ and 2 h of stirring returned the solution to a red color. The dichloromethane layer was separated and the aqueous layer was extracted with $CH_2Cl_2$ (4 x 50 mL). Then, the combined organic layers were washed with brine (3 x 50 mL) and dried over $MgSO_4$. The resulting solid was then recrystallized in hexanes to yield **1** as red crystals (13.6 g, 37.9 mmol, 72.2%). mp: 97-98 °C; $^1$H NMR (500 MHz, $CDCl_3$) δ 7.09 (t, 1H), 7.55 (d, 2H). $^{13}$C NMR (125 MHz, $CDCl_3$) δ 131.5, 131.0, 130.0, 109.0. LRMS (EI) m/z 361.8 ($M^+$), 234.9.

2,2',6,6'-Tetrabromo-biphenyl **(2)**. [10]

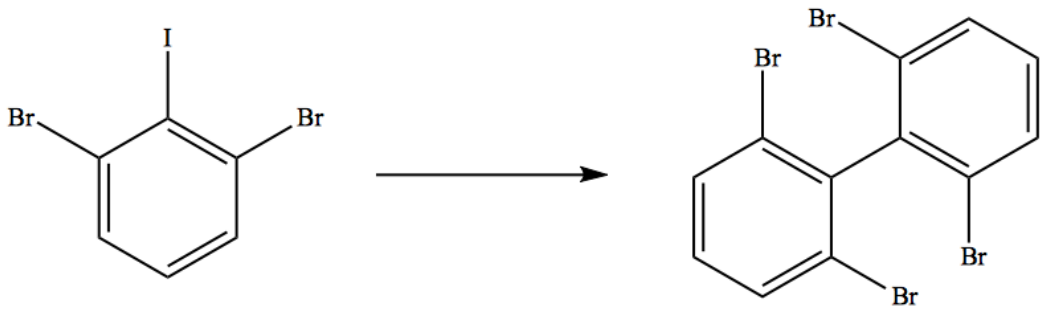


A solution of $^{n}$BuLi (2.5 M in hexanes, 43.2 mmol, 17.2 mL) was added dropwise to a maroon solution of 1,3-dibromo-2-iodobenzene (15.8 g, 43.6 mmol) in $Et_2O$ (300 mL) at -78 $^{o}$C. This mixture was stirred at -78 $^{o}$C for 2 h. Then, anhydrous $CuCl_2$ (17.4 g, 129 mmol) was added and stirred at -78 $^{o}$ C for 2h, producing a dark brown solution, before allowing the mixture to warm to room temperature. Cold water (300 mL) was added and the mixture was stirred until all brown residues disappeared. The ether layer was separated, and the aqueous layer was extracted with $Et_2O$ (3 x 250 mL) and toluene (100mL). The combined organic layers were dried over $Na_2SO_4$, and the solvent was evaporated. The resulting solid was recrystallized from boiling cyclohexane to afford **2** as a brown solid (2.2 g, 4.7 mmol, 22%). mp: 217-218 °C; $^{1}$H NMR (500 MHz, $CDCl_3$) δ 7.65 (d, 4H), 7.15 (t, 2H). $^{13}$C NMR (125 MHz, $CDCl_3$) δ 142.2, 132.0, 131.0, 124.2 LRMS (EI) m/z 469.8 ($M^+$), 388.8, 309.9, 150.0.

Subsequently, a more efficient procedure was adapted to synthesize 2,2',6,6'-tetrabromo-biphenyl as demonstrated below.

2,2',6,6'-Tetrabromo-biphenyl **(2)**. [10]

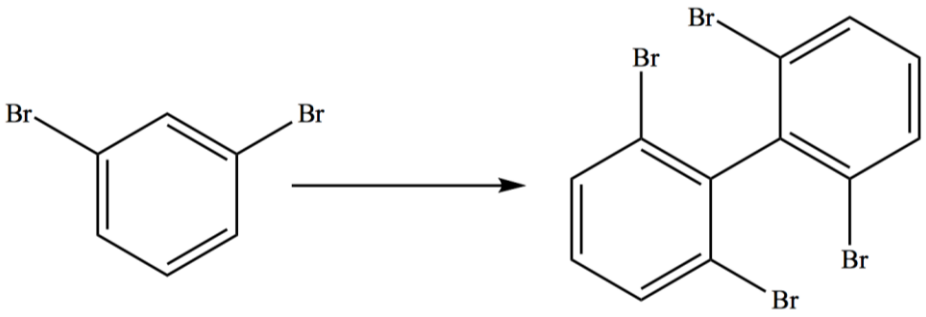


A solution of $^{n}$BuLi (2.5 M in hexanes, 57.5 mmol, 23 mL) was added over 10 min. to a degassed solution of diisopropylamine (7 mL, 50 mmol) and THF (100 mL) at -78 °C and stirred for 1 h. Then, 1,3 dibromobenzaldehyde (50 mmol, 6 mL) was added at the same temperature and stirred for 2 h, producing a milky yellow solution. Then, CuBr (3.6 g, 25 mmol) and LiCl (1.3 g, 30. mmol) were added and stirred for 2 h, instantly producing a turquoise hue. Subsequently, benzoquinone (8.2 g, 76 mmol) and THF (10 mL) were added and stirred for 1 h before the reaction mixture was warmed to room temperature overnight, producing a deep violet color. The reaction was quenched with distilled water (50 mL) and the aqueous layer was extracted with dichloromethane (3 x 50 mL). mp: 217-218 °C; $^{1}$H NMR (500 MHz, $CDCl_3$) δ 7.65 (d, 4H), 7.15 (t, 2H). $^{13}$C NMR (125 MHz, $CDCl_3$) δ 142.1, 132.1, 131.0, 124.2. LRMS (EI) m/z 469.8 ($M^+$), 388.8, 309.9, 150.0.

6,6'-dibromo-[1,1'-biphenyl]-2,2'-dicarbaldehyde **(3)**. [13]

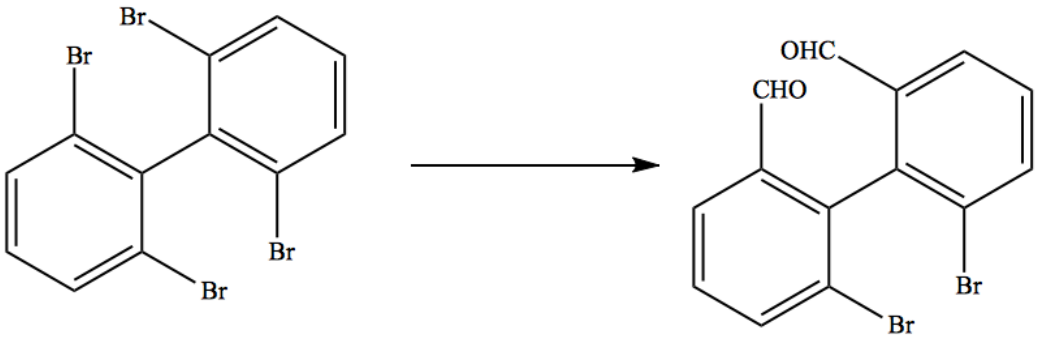


To a light brown solution of **2** (1.8 g, 3.9 mmol) in dry THF (350 mL), $^{n}$BuLi solution in hexanes (2.5 M, 7.35 mL, 18.3 mmol) was added at -78 °C under Argon, and the mixture was stirred for 2 h at -78 °C. Then, to this solution, N,N-dimethylformamide (1.4 mL, 18 mmol) was added and stirred 30 min at -78 °C. After addition of saturated $NH_4Cl$ (50 mL), the mixture was warmed up to room temperature over 1 h. The organic layer was isolated and the aqueous layer was extracted with EtOAc (3 x 50 mL). The combined organic layers were washed with 1 M HCl (2 x 50 mL) and brine (100 mL). Then, the organic layer was dried over $MgSO_4$ and filtered. The solvent was evaporated, and the crude product was purified by silica gel column chromatography to give the dialdehyde, **3**, as a yellow solid (477 mg, 1.29 mmol, 33.6%). mp: 117.5-122.5 °C $^{1}$H NMR (500 MHz, $CDCl_3$) δ 7.55 (t, 2H), 7.95 (d, 2H), 8.05 (d, 2H), 9.60 (s, 2H). $^{13}$C NMR (125 MHz, $CDCl_3$) δ 189.5, 140.1, 138.0, 136.0, 130.5, 128.5, 125.5. LRMS (EI) m/z 367.8 ($M^+$), 289.0, 259.0, 180.0.

4,5-dibromophenanthrene **(4).** [6]

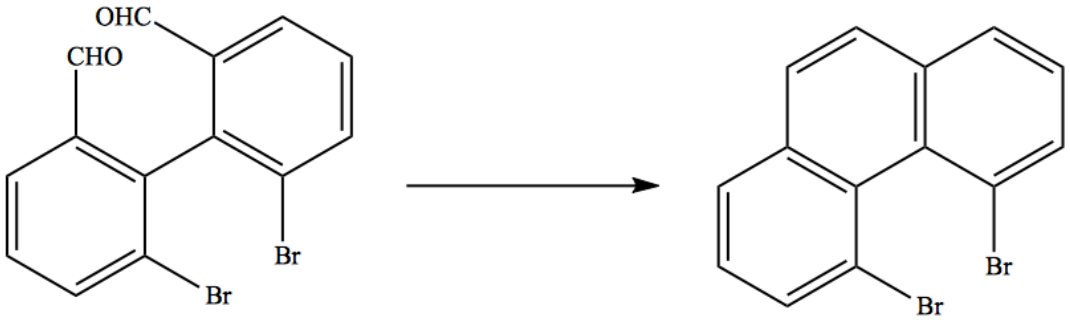


The dialdehyde compound, **3**, (107 mg, 0.291 mmol), p-toluenesulfonyl hydrazide (114 mg, 0.615 mmol), and toluene (2 mL) were successively added to a flame-dried flask under argon. The milky white mixture was heated at 60 °C and stirred for 10 min. Then, toluene (14 mL) was added, and the solution was cooled to room temperature. Then, 4 Å molecular sieves (100 mg), KOtBu (100. mg, 0.891 mmol), $Rh_2(OAc)_4$ (2 mg, 0.0045 mmol), and toluene (14 mL) were added successively. The reaction system was degassed with argon and the resulting solution was stirred at 90 °C for 1 h, producing a deep brown-red color after 20 min. The mixture was then cooled to room temperature and the crude product was purified by silica gel column chromatography to give **4**, as colorless crystals (24 mg, 0.071 mmol, 24%). mp: 170-171 °C; $^1$H NMR (500 MHz, $CDCl_3$) δ 7.40 (m, 1H), 7.50 (m, 1H), 7.70 (m, 1H), 7.80 (m, 1H). $^{13}$C NMR (125 MHz, $CDCl_3$) δ 135.0, 132.1, 129.2, 128.0, 127.0, 126.0, 122.1. LRMS (EI) m/z 335.9 ($M^+$), 255, 176.

4-bromo-5-*tert*-butylphenanthrene **(5b).** [9]

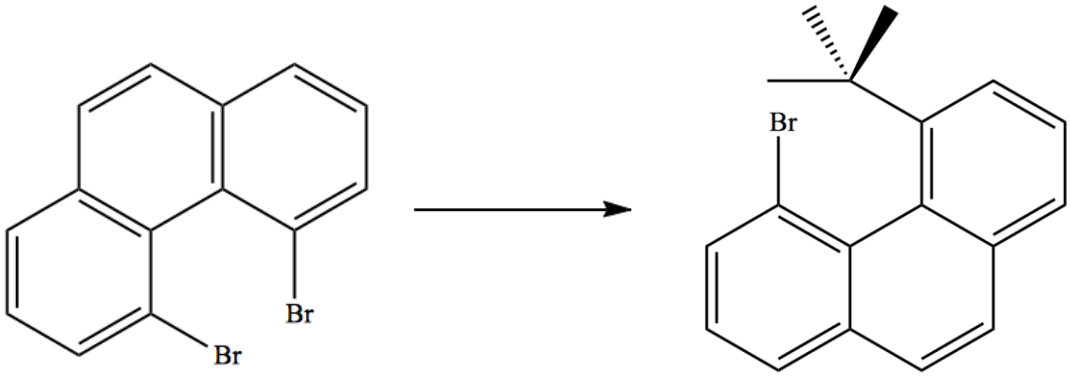


To a degassed mixture of **4** (57 mg, 0.16 mmol) and $NiCl_2 \bullet (H_2O)_{1.5}$ (2.7 mg, 0.017 mmol) and 1,3-bis(cyclohexyl)imidazolium tetrafluoroborate (5.4 mg, 0.016 mmol), a solution of *t*-BuMgCl (1M in THF, 0.68 mL, 0.68 mmol) was slowly added at -10 $^{o}$C, producing a light yellow color. The mixture was stirred for 2 h, inducing a color change to a dark forest green. Ice chips were added to quench the reaction, and after the mixture warmed to room temperature, a solution of saturated $NH_4Cl$ (10 mL) was added. Then, the aqueous layer was extracted with ethyl acetate (3 x 10 mL), and the combined organic layers were washed with brine (10 mL). The isolated organic layer was then dried over $Na_2SO_4$. The crude product was then purified by silica gel column chromatography. LRMS (EI) m/z 312.0, 314.0 ($M^+$).

*Computational Procedures*

All geometry and optimization calculations were performed using Becke's three parameter hybrid density correlation functional of density functional theory (DFT) established by Lee, Yang, and Parr (B3LYP) on Gaussian 09.[15] The 6-31G(d) basis set was used for all geometry optimization and frequency calculations. Dihedral angles were measured between C4 and C5 for all phenanthrene molecules.

Transition state calculations were carried out with QST2 optimizations on the optimized enantiomers of **4, 5, 5b**, and **6** with the B3LYP/6-31G(d) method, but only that for **4** was possible. These calculations were followed up with frequency calculations to confirm imaginary normal modes of each transition state.

# References


[1] Carey, F.A.; Sundberg, R.J. *Advanced Organic Chemistry Part B: Reactions and Synthesis* (4th Edition). Kluwer Academic/ Plenum Publishers: New York, 2001.

[2] Zhong, Y., Carmella, S. G., Upadhyaya, P., Hochalter, J. B., Rauch, D., Oliver, A., Hecht, S. S. (2011). Immediate Consequences of Cigarette Smoking: Rapid Formation of Polycyclic Aromatic Hydrocarbon Diol Epoxides. Chemical Research in Toxicology, 24(2), 246-252.

[3] Mallory, F.B.; Wood, C.S.; Gordon, J.T. Photochemistry of Stilbenes. III. Some Aspects of the Mechanism of Photocyclization to Phenanthrenes. *J.Am.Chem.Soc.* **1964,** *86*, 3094-3102.

[4] Liu, L. B.; Yang, B. W.; Katz, T.J.; Poindexter, M. K. Improved Methodology for Photocyclization Reactions. *J. Org. Chem.* **1991**, *56*, 3769-3775.

[5] Sudhakar, A.; Katz, T.J. Directive Effect of Bromine on Stilbene Photocyclizations. An improved synthesis of [7]helicenes. *Tetrahedron Lett.* **1986**, *27*, 2231-2234.

[6] Xia Y.; Liu, Z.; Xiao, Q.; Qu, P.; Ge, R.; Zhang, Y.; Wang, J. Rhodium(II)-Catalyzed Cyclization of Bis(N-tosylhydrazone)s: An Efficient Approach towards Polycyclic Aromatic Compounds. *Angew. Chem. Int. Ed.* **2012**, *51*, 5714-5717.

[6a] Shen, Y., & Chen, C.-F. (2012). Helicenes: Synthesis and Applications. *Chemical Reviews, 112*(3), 1463-1535.

[6b] Flammang., M; Nasielsk., J; Martin, R. H. Tetrahedron Lett. 1967, 8, 743.

[6c] Zhang, Y. Z.; Petersen, J. L.; Wang, K. K. Org. Lett. 2007, 9, 1025.

[7] Scheriibl, H.; Fritzche, U.; Mannschreck, A. Synthesis, Chromatic Enrichment of Enantiomers and Barriers to Enantiomerization of Helical Phenanthrenes. **1984**, *343*, 336-343.

[8] Shaum, J. The Feud in the Fjord: The Generation of Twisted Phenanthrenes. Honors Thesis, Colby College, Waterville, ME, 2013.

[9] Biscoe, M., et al. Nickel-Catalyzed Kumada Cross-Coupling Reactions of Tertiary Alkylmagnesium Halides and Aryl Bromides/Triflates. *J. Am. Chem. Soc.* **2011,** 133(22): 8478-8481.

[10] Perron, Q., et al. Chiral bromine–lithium exchange catalyzed by diamines. *Tetrahedron: Asymmetry.* **2009,** 20(9): 1004-1007.

[11] Cosmo, R., Hambley, T. W., & Stermhell, S; Anomalous Internuclear Distances in 1,8-Substituted Naphthalenes and 1,4-Substituted Phenanthrenes. *Tetrahedron Letters.* **1987**, *28* (49), 6239-6240.

[12] Kilyanek, S.; Fang, X.; Jordan, R.; Synthesis and Reactivity of a Tetragallium Macrocycle. *Organometallics.* **2009,** *28* (1), 300-305.

[13] Suzuki, T.; Yoshimoto, Y.; Takeda, T.; Kawai, H.;Fujiwara, K., Intramolecular Methylacridan–Methylacridinium Complexes with a Phenanthrene-4,5-diyl or Related Skeleton: Geometry–Property Relationships in Isolable C[BOND]H Bridged Carbocations. *Chem. Eur. J.*, **2009**, 15: 2210–2216.

[14] Foresman, J. B., & Frisch, Æ. (2015). Exploring chemistry with electronic structure methods. 3rd ed. Pittsburgh, Pa: Gaussian.

[15] Gaussian 09, Revision A.02, M. J. Frisch, G. W. Trucks, H. B. Schlegel, G. E. Scuseria, M. A. Robb, J. R. Cheeseman, G. Scalmani, V. Barone, B. Mennucci, G. A. Petersson, H. Nakatsuji, M. Caricato, X. Li, H. P. Hratchian, A. F. Izmaylov, J. Bloino, G. Zheng, J. L. Sonnenberg, M. Hada, M. Ehara, K. Toyota, R. Fukuda, J. Hasegawa, M. Ishida, T. Nakajima, Y. Honda, O. Kitao, H. Nakai, T. Vreven, J. A. Montgomery, Jr., J. E. Peralta, F. Ogliaro, M. Bearpark, J. J. Heyd, E. Brothers, K. N. Kudin, V. N. Staroverov, R. Kobayashi, J. Normand, K. Raghavachari, A. Rendell, J. C. Burant, S. S. Iyengar, J. Tomasi, M. Cossi, N. Rega, J. M. Millam, M. Klene, J. E. Knox, J. B. Cross, V. Bakken, C. Adamo, J. Jaramillo, R. Gomperts, R. E. Stratmann, O. Yazyev, A. J. Austin, R. Cammi, C. Pomelli, J. W. Ochterski, R. L. Martin, K. Morokuma, V. G. Zakrzewski, G. A. Voth, P. Salvador, J. J. Dannenberg, S. Dapprich, A. D. Daniels, O. Farkas, J. B. Foresman, J. V. Ortiz, J. Cioslowski, and D. J. Fox, Gaussian, Inc., Wallingford CT, 2009.

# Appendix A: Spectral Data (GC/MS, NMR, Melting Point, IR, X-Ray Data)

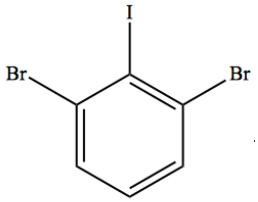


**1**



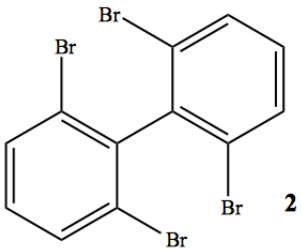


**2**



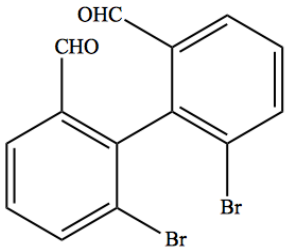


**3**



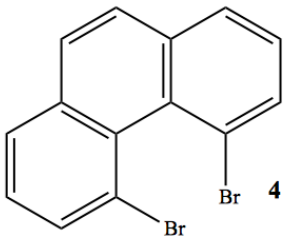


**4**



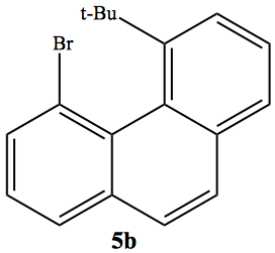


**5b**

GC/MS spectrum for 1,3-dibromo-2-iodobenzene **(1)**

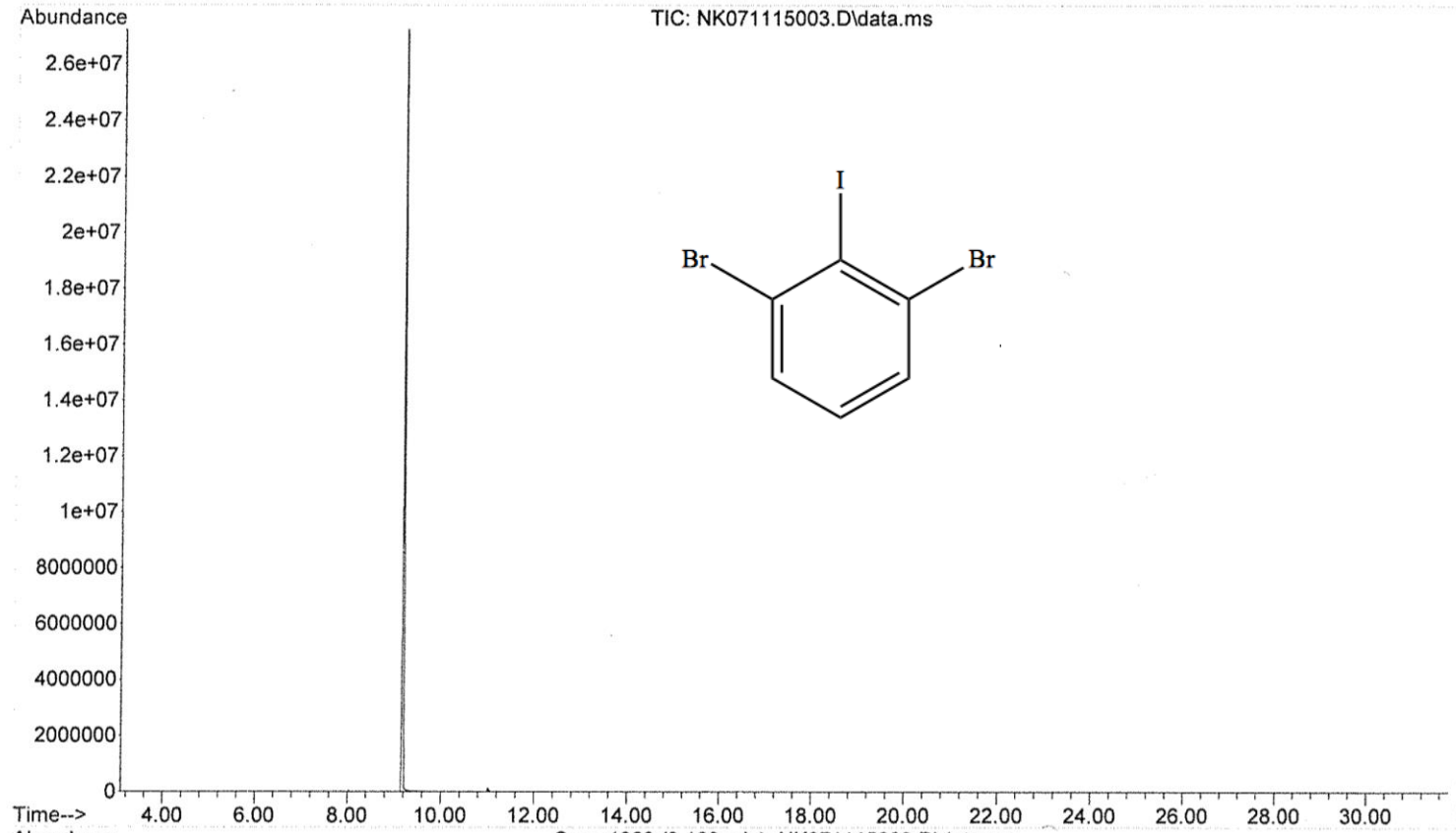


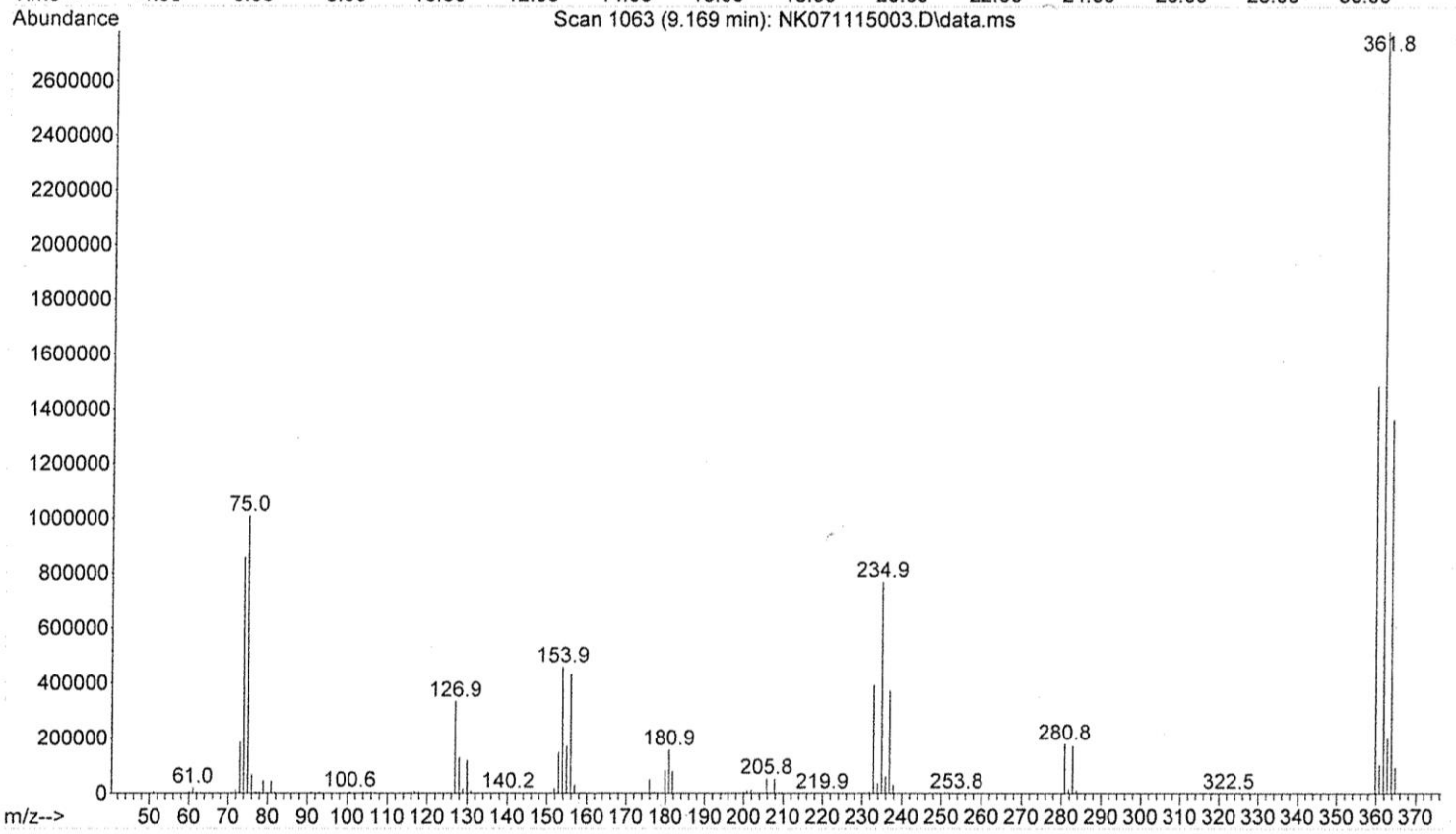

$^{1}$H NMR spectrum for 1,3-dibromo-2-iodobenzene in $CDCl_3$ **(1)**

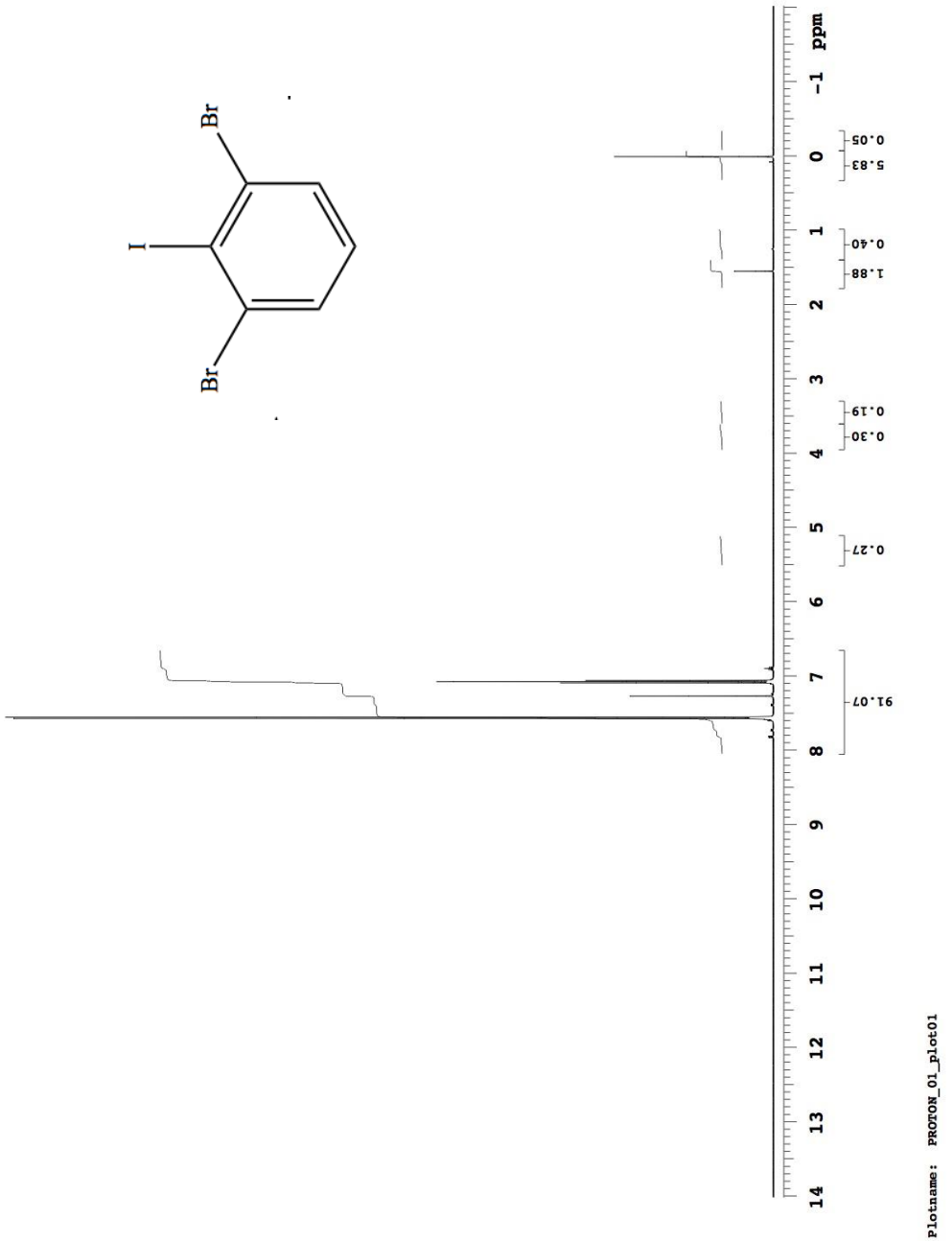

$^{13}C$ NMR spectrum for 1,3-dibromo-2-iodobenzene in $CDCl_3$ **(1)**

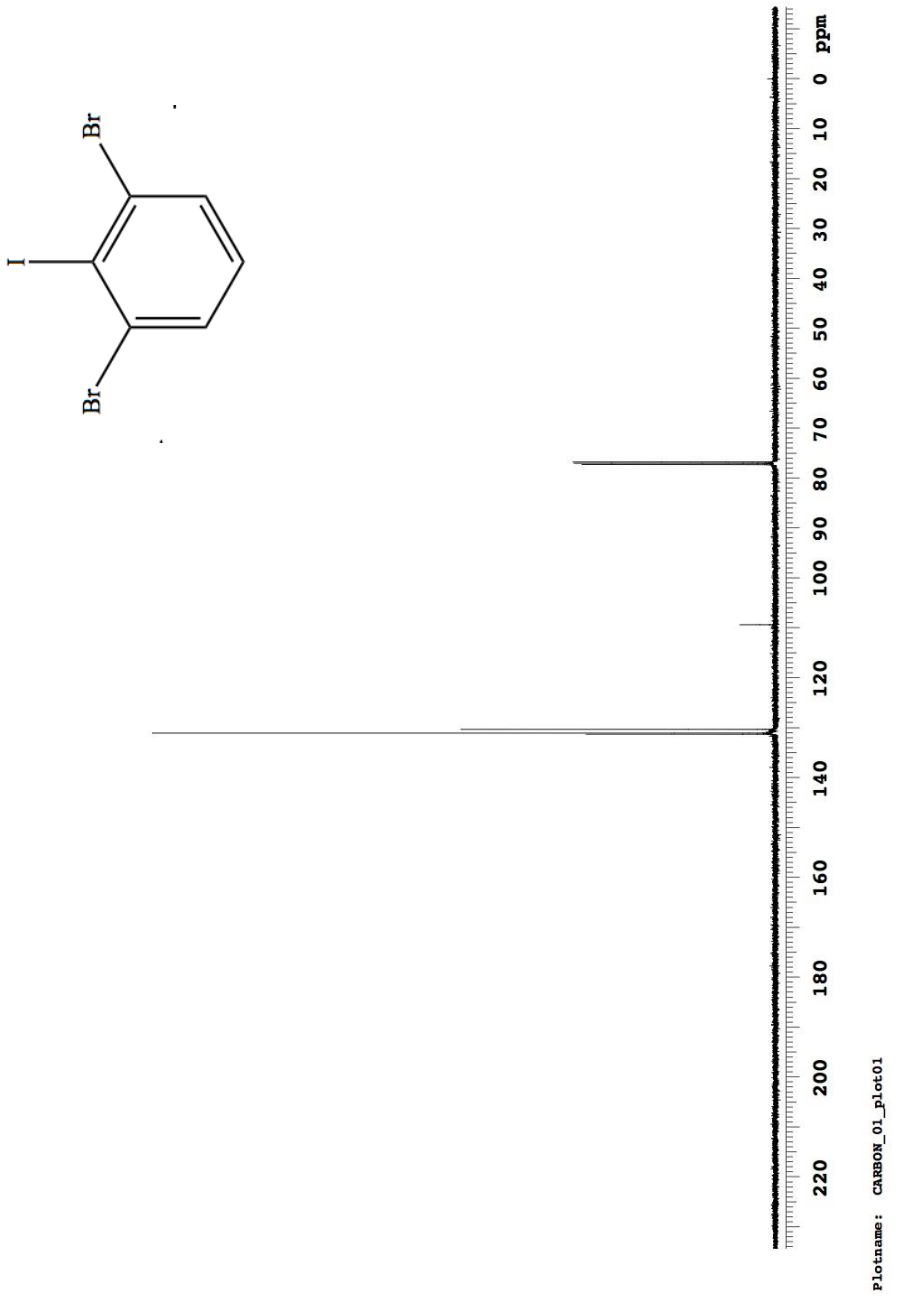

GC/MS spectrum for 2,2',6,6'-Tetrabromo-biphenyl **(2)**

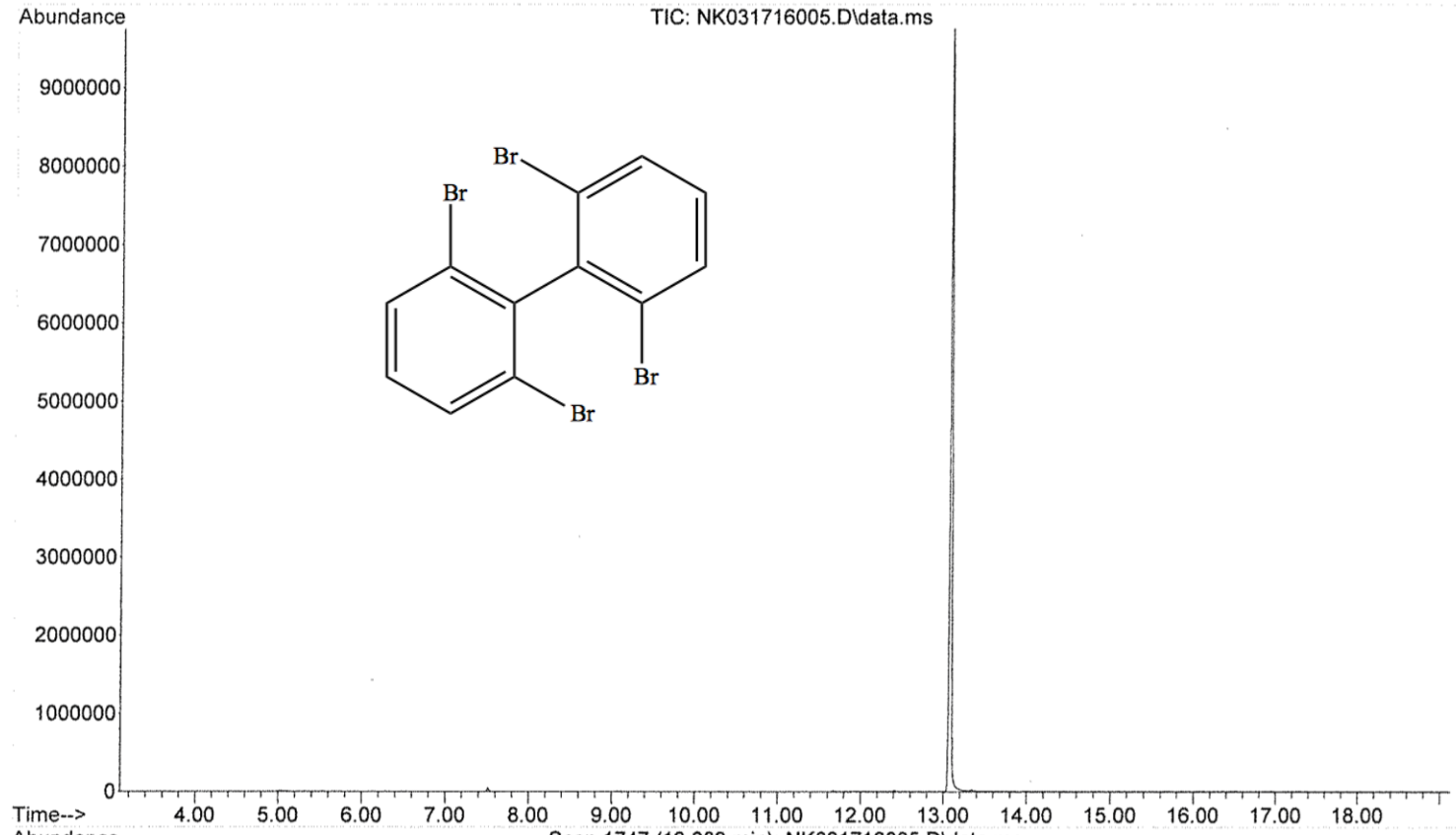


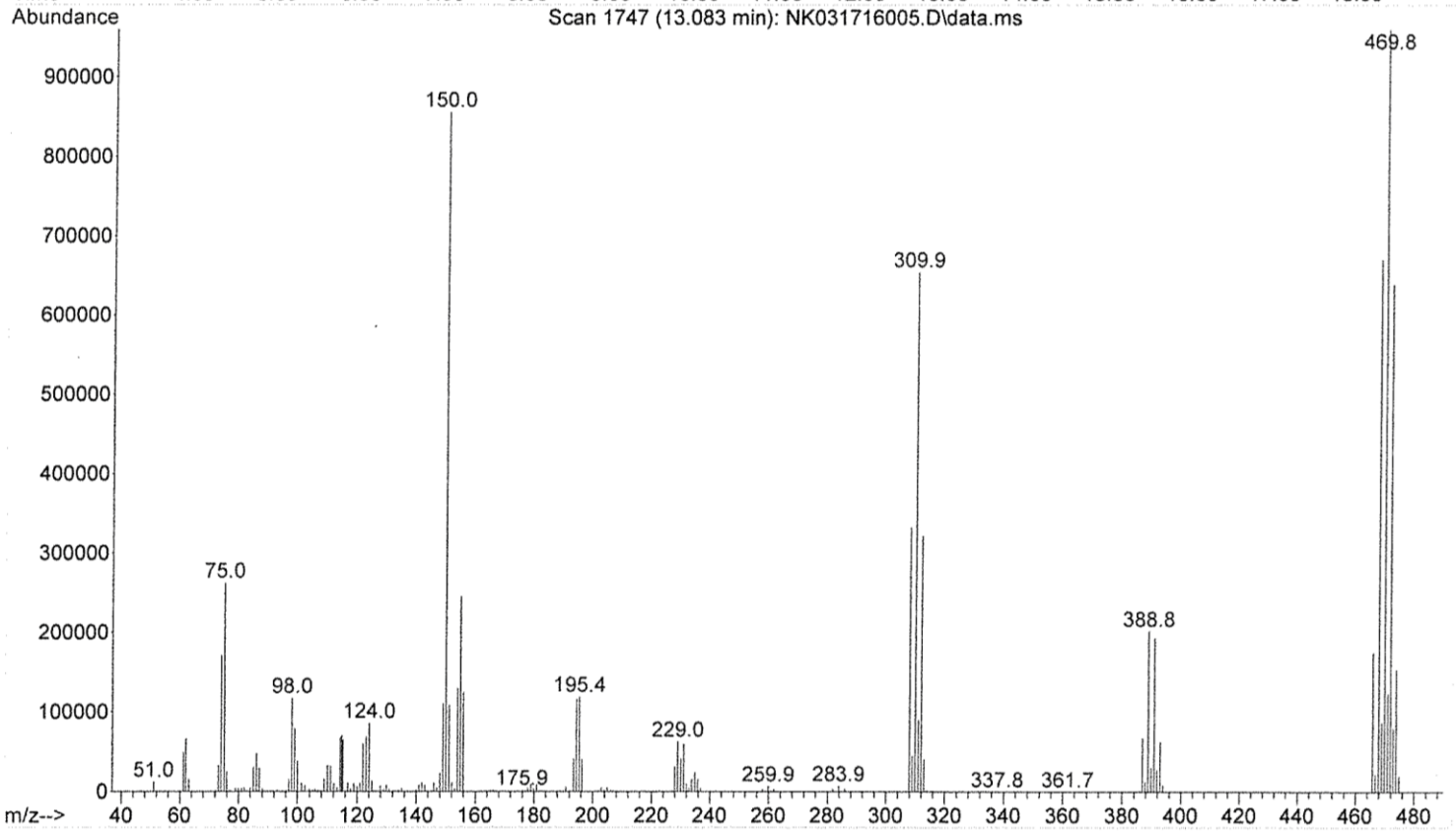

$^{1}$H NMR spectrum for 2,2',6,6'-Tetrabromo-biphenyl in $CDCl_3$ **(2)**

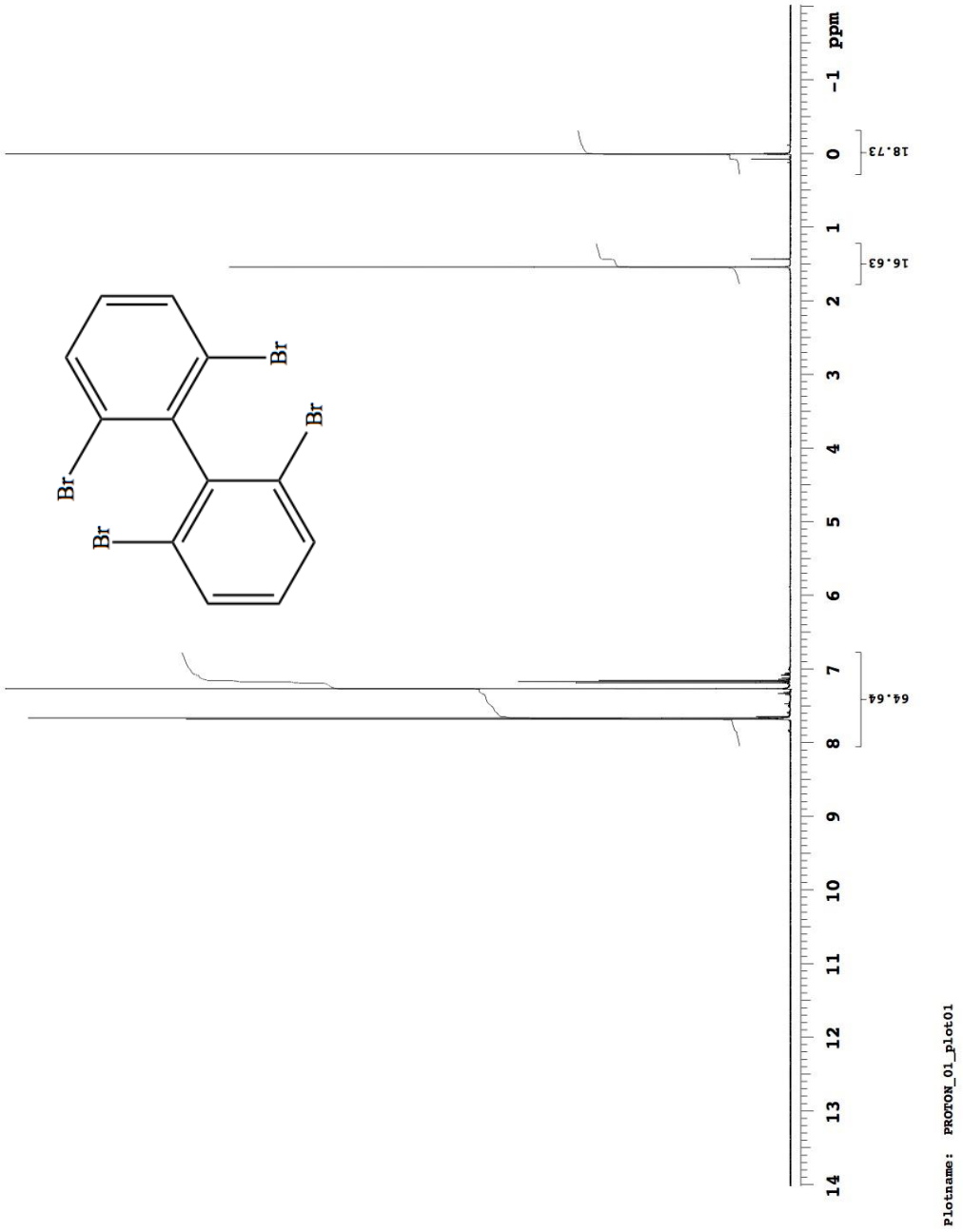

$^{13}C$ NMR spectrum for 2,2',6,6'-Tetrabromo-biphenyl in $CDCl_3$ **(2)**

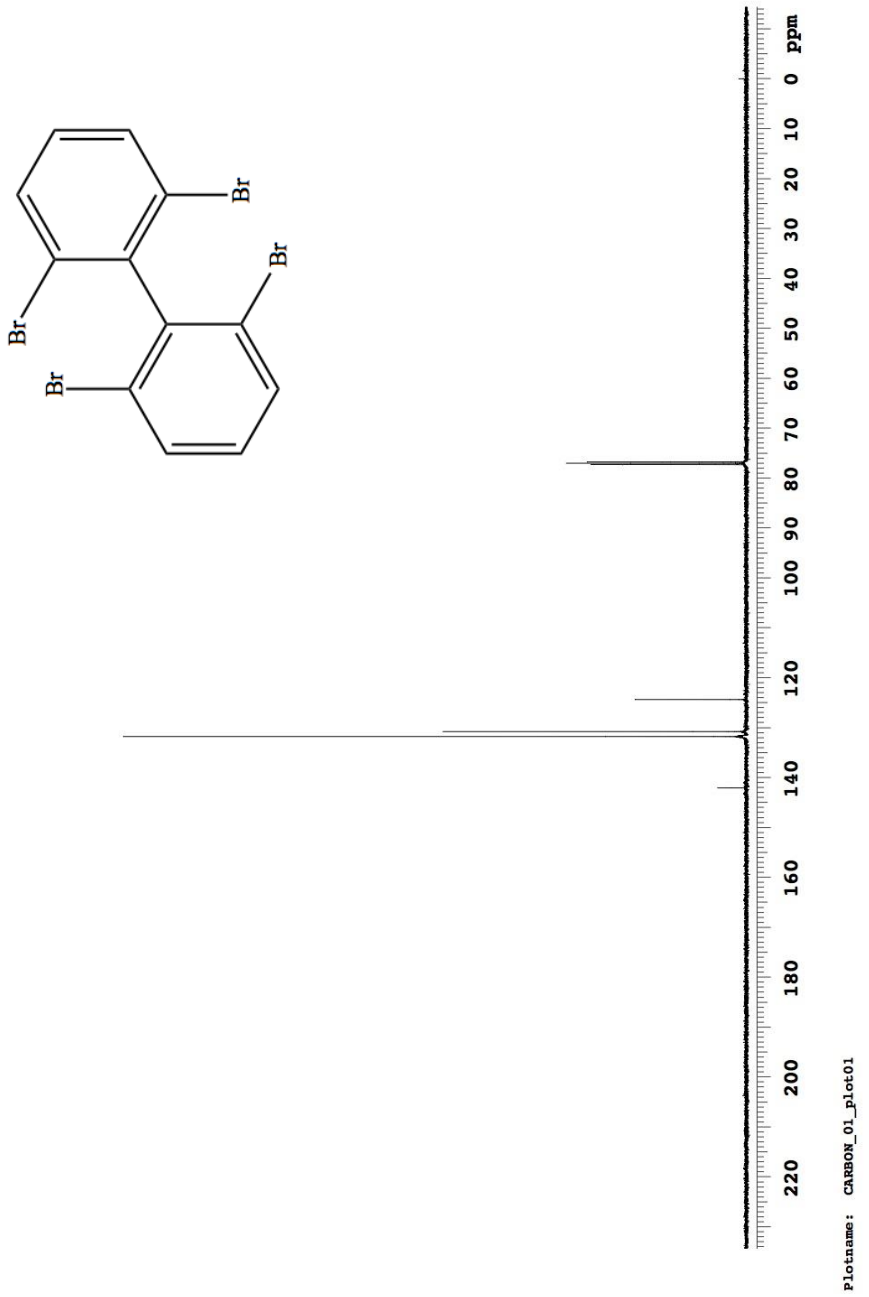

GC/MS spectrum for 6,6'-dibromo-[1,1'-biphenyl]-2,2'-dicarbaldehyde **(3)**

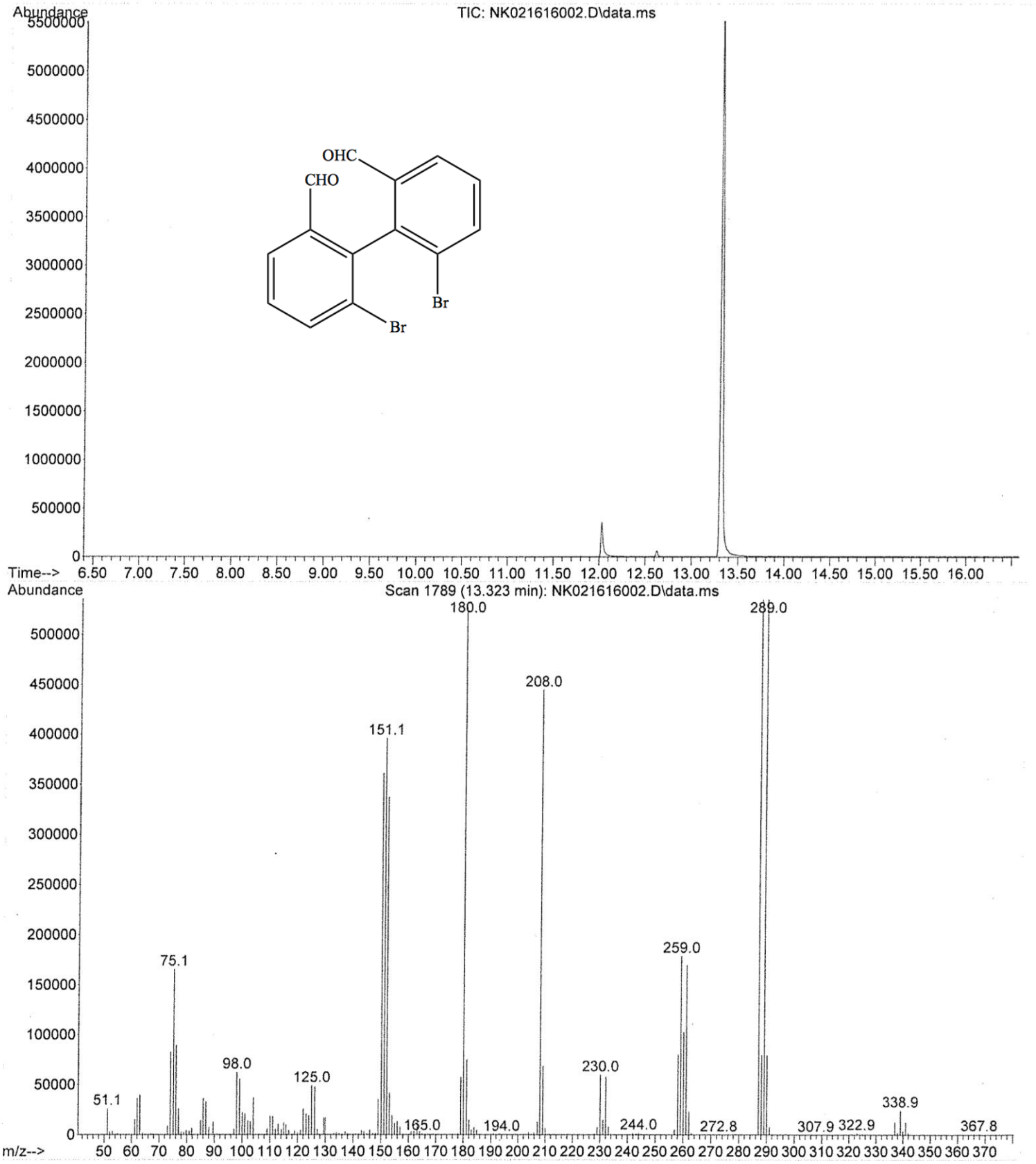

$^{1}$H NMR spectrum for 6,6'-dibromo-[1,1'-biphenyl]-2,2'-dicarbaldehyde in $CDCl_3$ **(3)**

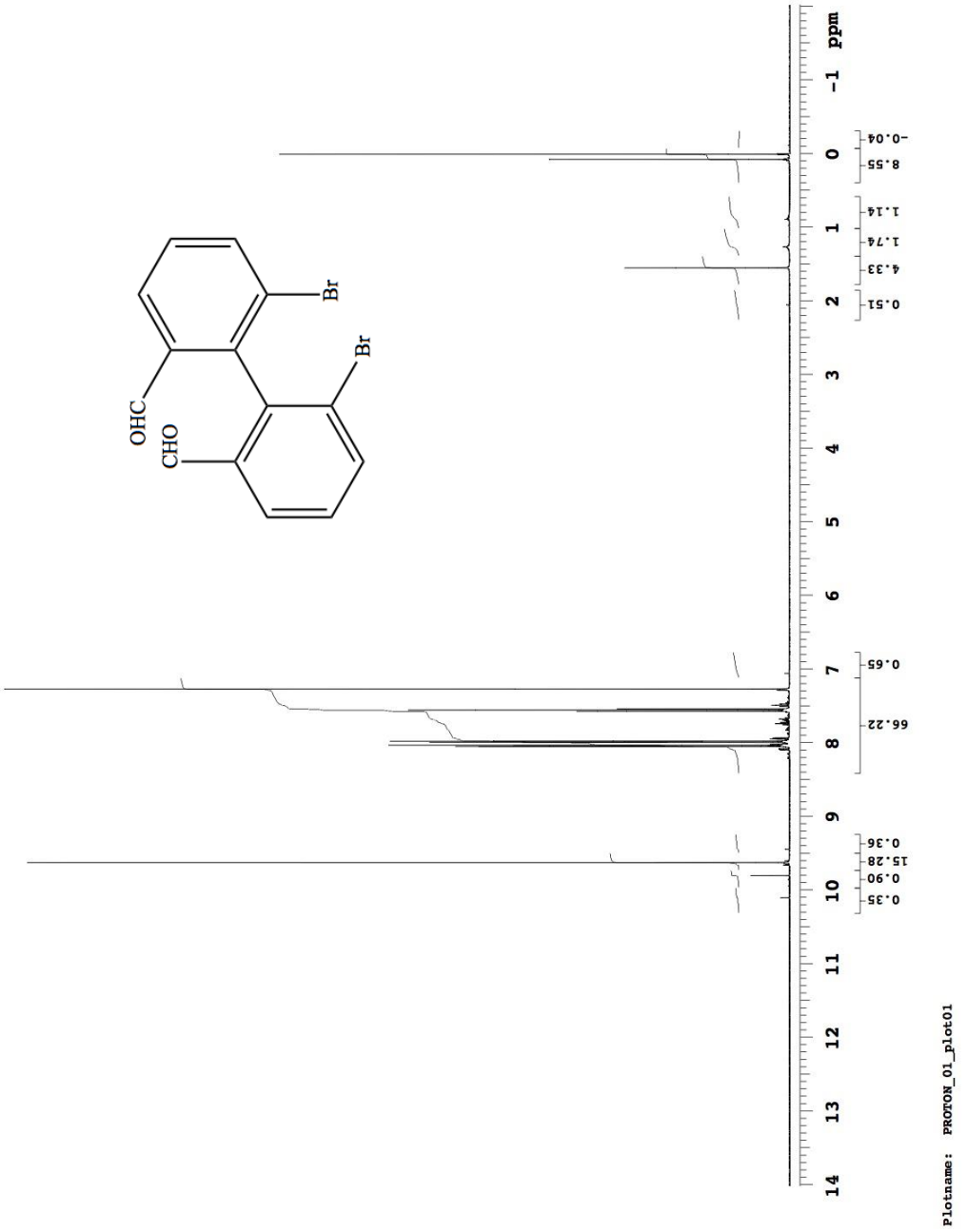

$^{13}C$ NMR spectrum for 6,6'-dibromo-[1,1'-biphenyl]-2,2'-dicarbaldehyde in $CDCl_3$ **(3)**

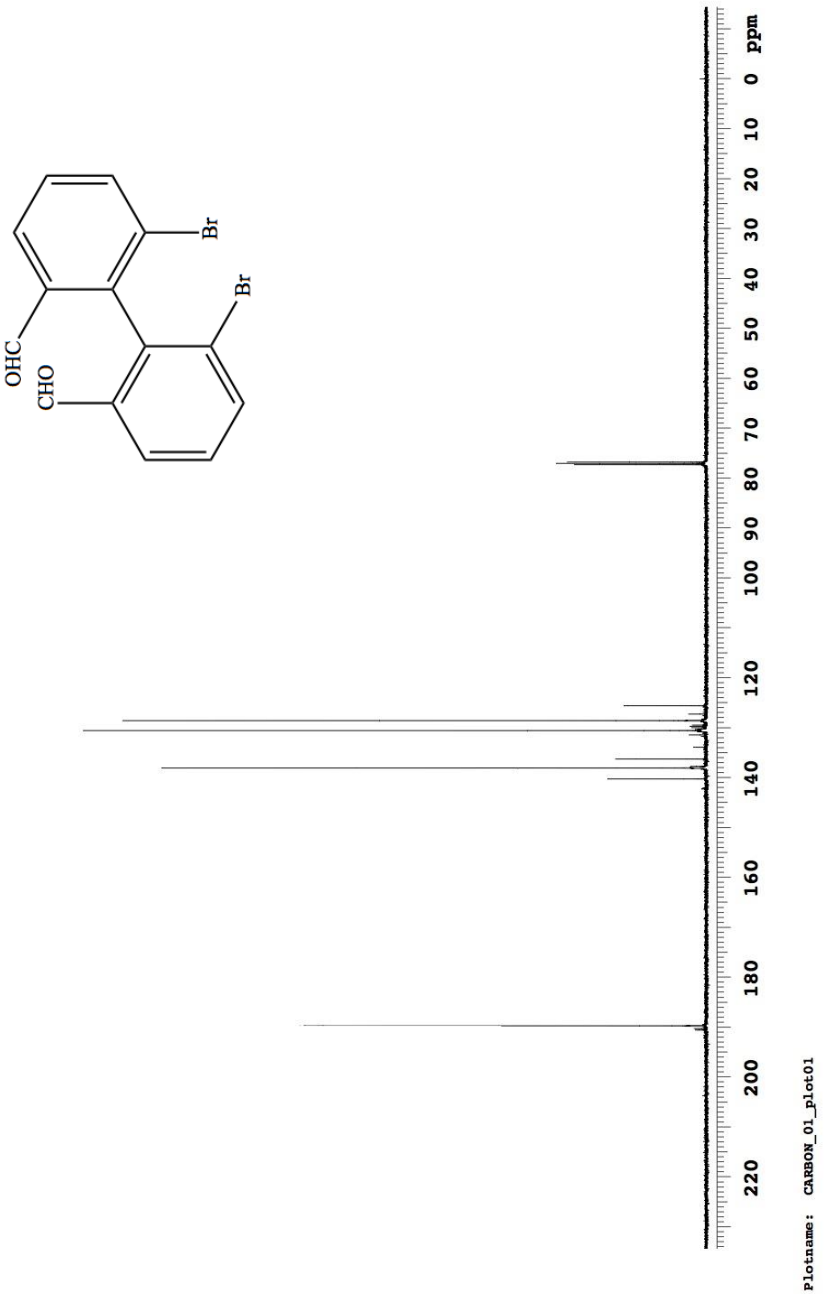

GC/MS spectrum for 4,5-dibromophenanthrene **(4)**

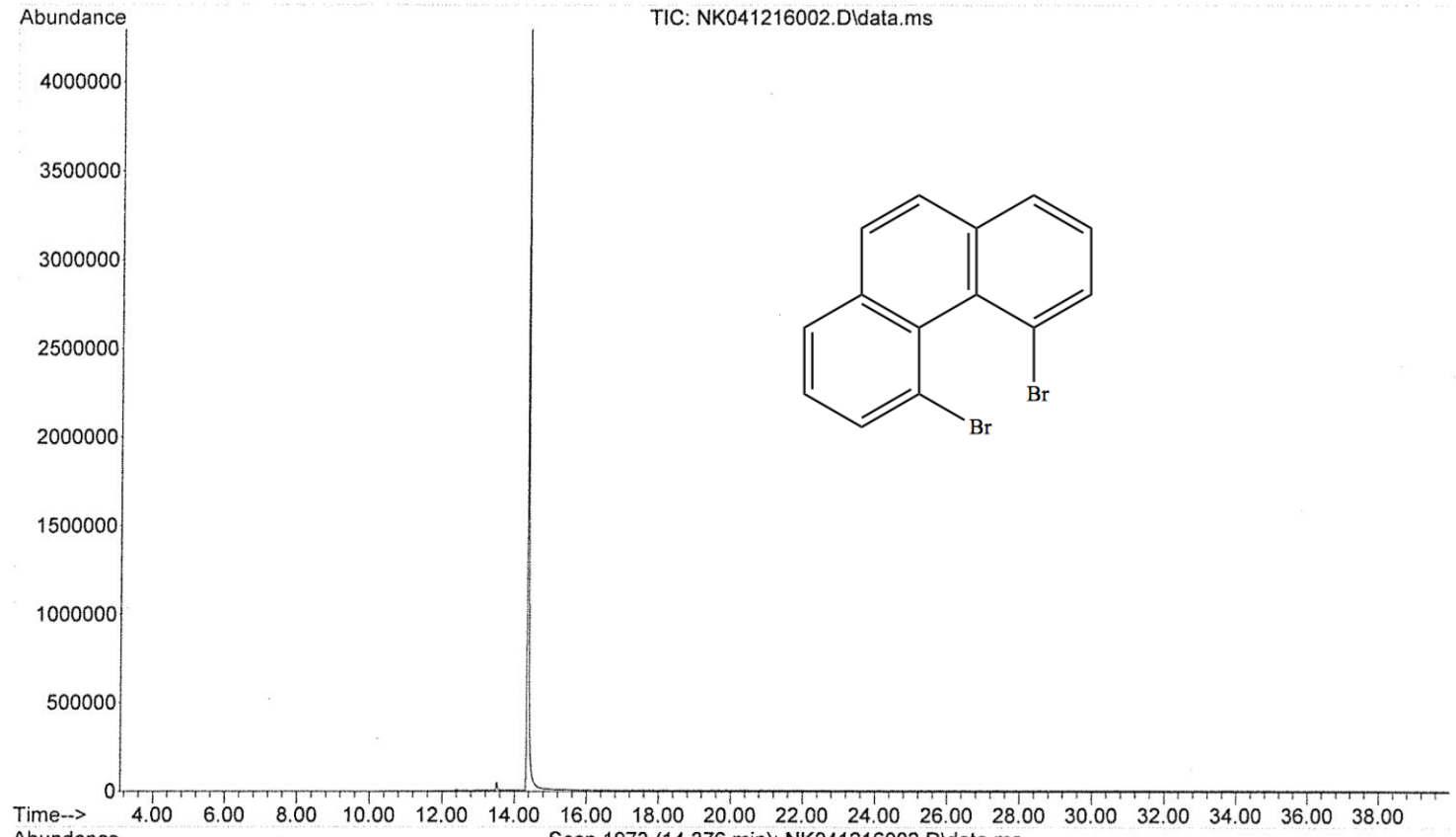


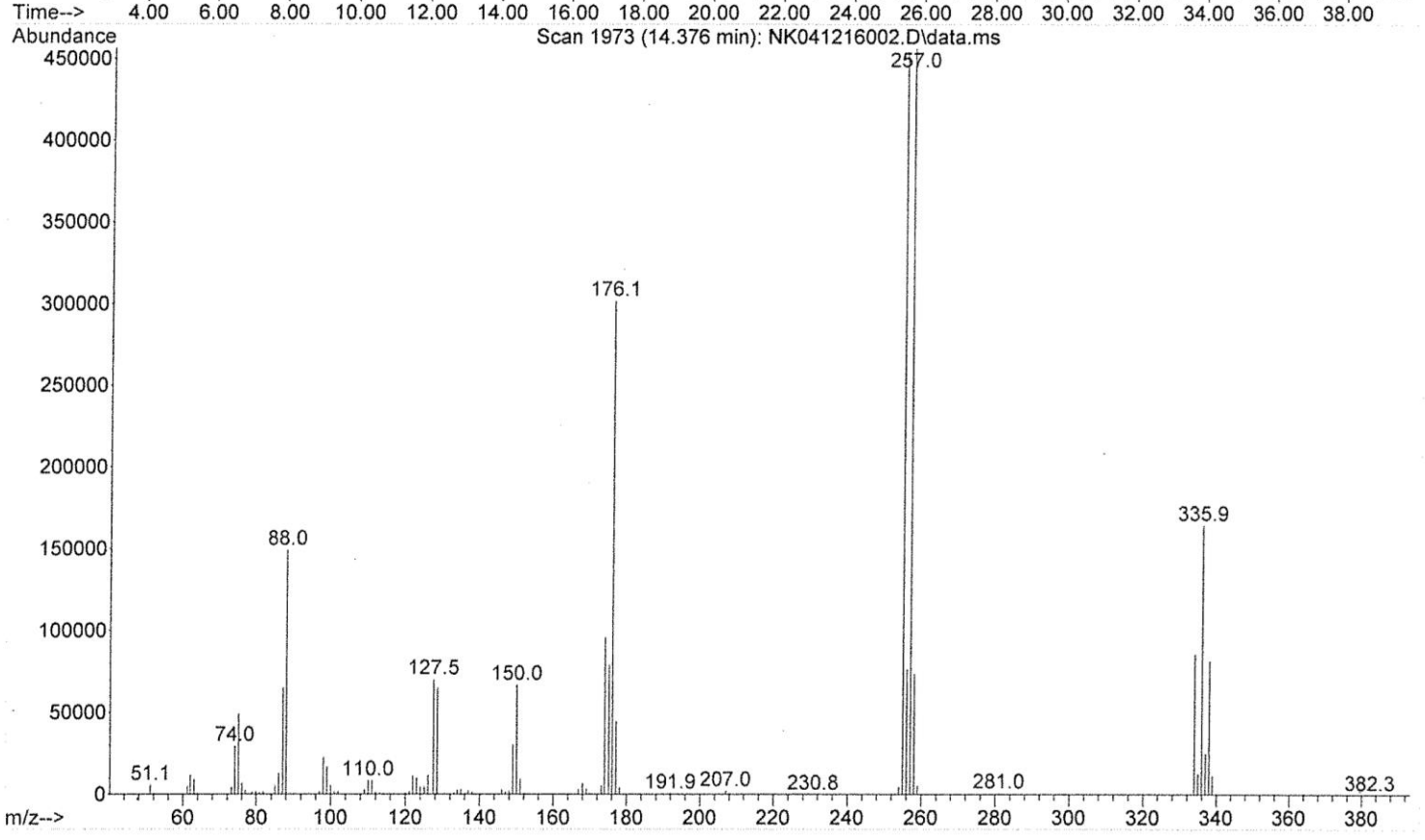

$^{1}H$ NMR spectrum for 4,5-dibromophenanthrene in $CDCl_3$ **(4)**

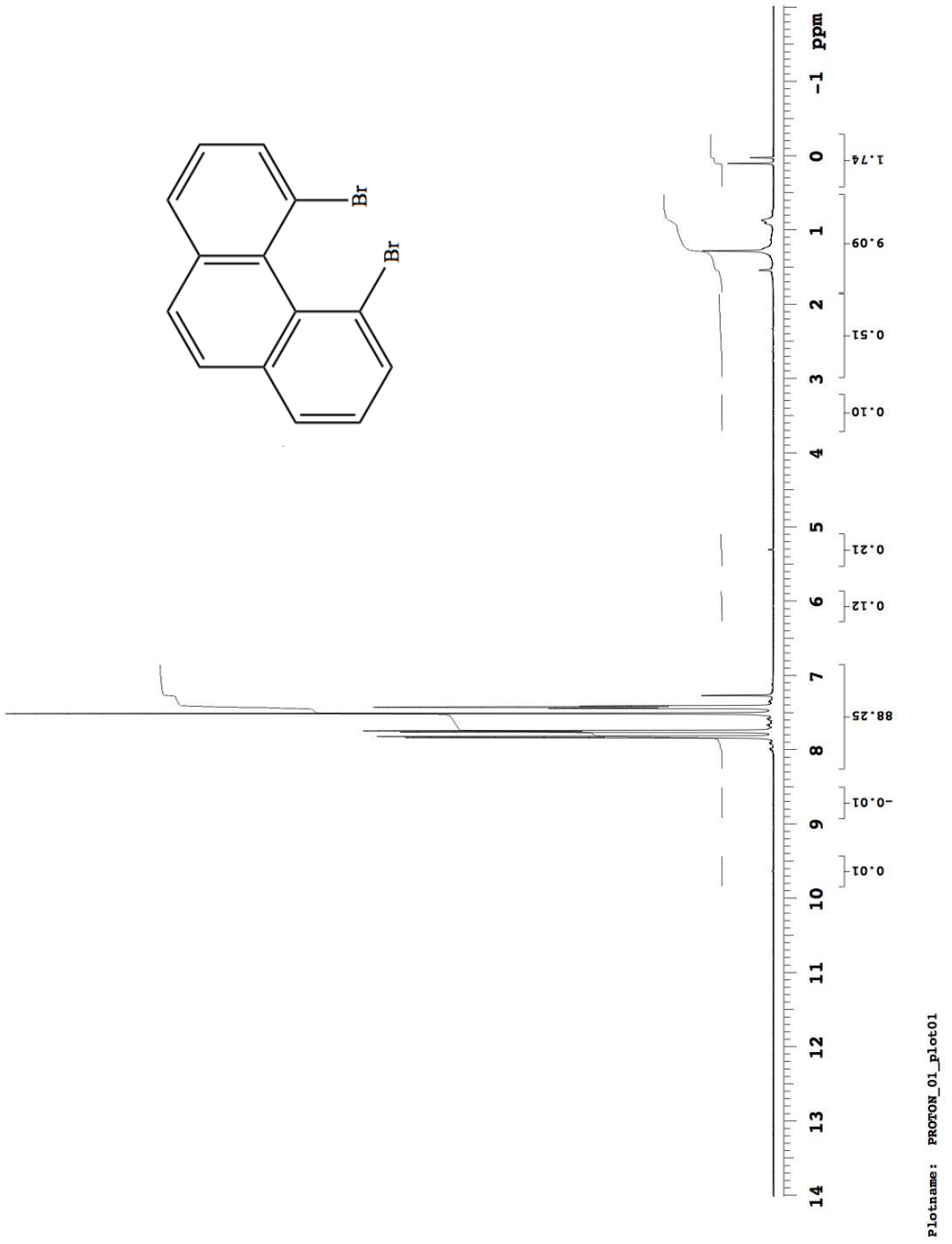

$^{13}C$ NMR spectrum for 4,5-dibromophenanthrene in $CDCl_3$ **(4)**

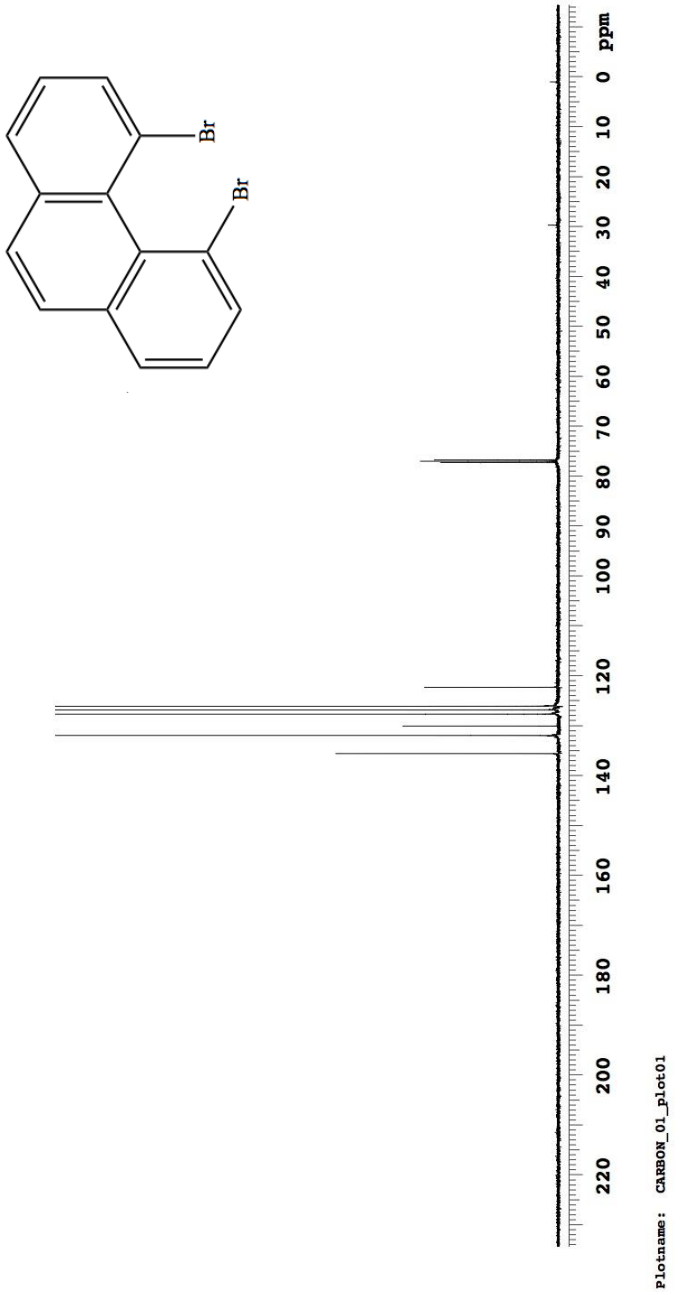

IR spectrum for 4,5-dibromophenanthrene **(4)**

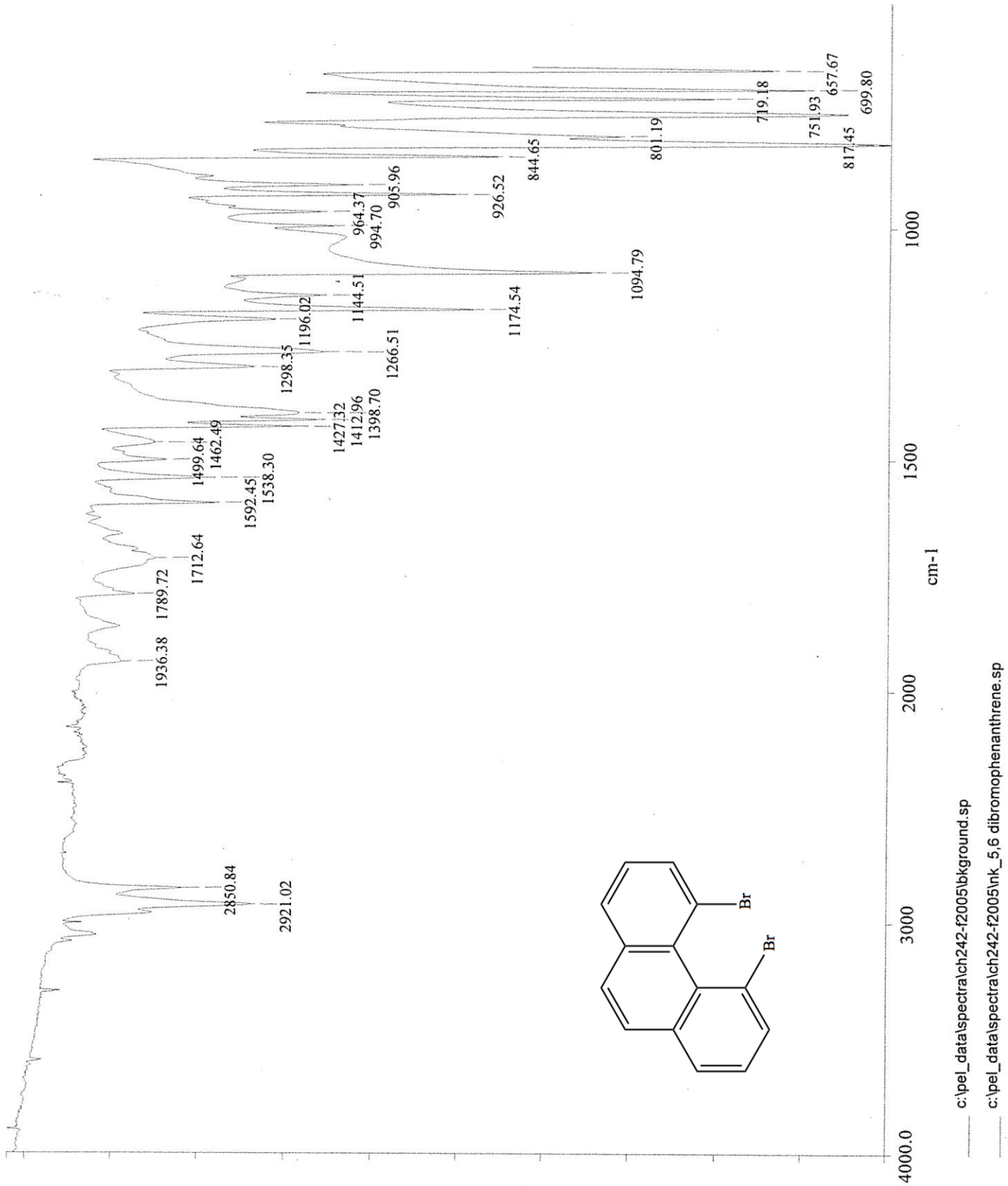

Crystal Structure Report for 4,5-dibromophenanthrene **(4)**

A clear colourless block hexago-like specimen of $C_7H_5Br$, approximate dimensions 0.070 mm x 0.110 mm x 0.250 mm, was used for the X-ray crystallographic analysis. The X-ray intensity data were measured.

The total exposure time was 10.27 hours. The frames were integrated with the Bruker SAINT software package using a narrow-frame algorithm. The integration of the data using a monoclinic unit cell yielded a total of 4359 reflections to a maximum θ angle of 26.45° (0.80 Å resolution), of which 1171 were independent (average redundancy 3.722, completeness = 99.6%, $R_{int}$ = 1.81%, $R_{sig}$ = 1.58%) and 1043 (89.07%) were greater than $2\sigma(F^2)$. The final cell constants of a = 16.812(3) Å, b = 8.6002(13) Å, c = 8.1323(12) Å, β = 103.745(2)°, volume = 1142.1(3) $Å^3$, are based upon the refinement of the XYZ-centroids of 2282 reflections above 20 σ(I) with 4.988° < 2θ < 52.89°. Data were corrected for absorption effects using the multi-scan method (SADABS). The ratio of minimum to maximum apparent transmission was 0.710. The calculated minimum and maximum transmission coefficients (based on crystal size) are 0.2710 and 0.6380.

The final anisotropic full-matrix least-squares refinement on $F^2$ with 73 variables converged at R1 = 2.41%, for the observed data and wR2 = 6.39% for all data. The goodness-of-fit was 1.101. The largest peak in the final difference electron density synthesis was 0.625 $e^-/Å^3$ and the largest hole was -0.247 $e^-/Å^3$ with an RMS deviation of 0.087 $e^-/Å^3$. On the basis of the final model, the calculated density was 1.966 $g/cm^3$ and F(000), 656 $e^-$.

**Table 1**. Sample and crystal data for **4**.

| | | |
|---|---|---|
| Identification code | 4 | |
| Chemical formula | $C_7H_5Br$ | |
| Formula weight | 169.02 g/mol | |
| Temperature | 173(2) K | |
| Wavelength | 0.71073 Å | |
| Crystal size | 0.070 x 0.110 x 0.250 mm | |
| Crystal habit | clear colourless block hexago | |
| Crystal system | monoclinic | |
| Space group | C 1 2/c 1 | |
| Unit cell dimensions | a = 16.812(3) Å | α = 90° |
| | b = 8.6002(13) Å | β = 103.745(2)° |
| | c = 8.1323(12) Å | γ = 90° |
| Volume | 1142.1(3) $Å^3$ | |
| Z | 8 | |
| Density (calculated) | 1.966 $g/cm^3$ | |
| Absorption coefficient | 7.063 $mm^{-1}$ | |
| F(000) | 656 | |

**Table 2**. Data collection and structure refinement for **4**.

| | | |
|---|---|---|
| Theta range for data collection | 2.49 to 26.45° | |
| Index ranges | -20<=h<=20, -10<=k<=10, -9<=l<=10 | |
| Reflections collected | 4359 | |
| Independent reflections | 1171 [R(int) = 0.0181] | |
| Coverage of independent reflections | 99.6% | |
| Absorption correction | multi-scan | |
| Max. and min. transmission | 0.6380 and 0.2710 | |
| Refinement method | Full-matrix least-squares on $F^2$ | |
| Refinement program | SHELXL-2014/7 (Sheldrick, 2014) | |
| Function minimized | $\Sigma\, w(F_o^2 - F_c^2)^2$ | |
| Data / restraints / parameters | 1171 / 0 / 73 | |
| Goodness-of-fit on $F^2$ | 1.101 | |
| Final R indices | 1043 data; $I>2\sigma(I)$ | R1 = 0.0241, wR2 = 0.0614 |
| | all data | R1 = 0.0288, wR2 = 0.0639 |
| Weighting scheme | $w=1/[\sigma^2(F_o^2)+(0.0368P)^2+1.4188P]$ where $P=(F_o^2+2F_c^2)/3$ | |
| Largest diff. peak and hole | 0.625 and -0.247 eÅ$^{-3}$ | |
| R.M.S. deviation from mean | 0.087 eÅ$^{-3}$ | |

**Table 3**. Atomic coordinates and equivalent isotropic atomic displacement parameters (Å$^2$) for **4**.

U(eq) is defined as one third of the trace of the orthogonalized $U_{ij}$ tensor.

| | x/a | y/b | z/c | U(eq) |
|---|---|---|---|---|
| Br1 | 0.41184(2) | 0.94244(3) | 0.60763(3) | 0.03213(12) |
| C1 | 0.31148(17) | 0.6252(4) | 0.8762(4) | 0.0376(7) |
| C2 | 0.33324(16) | 0.7628(3) | 0.8066(3) | 0.0324(6) |
| C3 | 0.40451(15) | 0.7693(3) | 0.7505(3) | 0.0254(5) |
| C4 | 0.45980(15) | 0.6426(3) | 0.7685(3) | 0.0238(5) |
| C5 | 0.42911(16) | 0.4985(3) | 0.8160(3) | 0.0273(5) |
| C6 | 0.35698(17) | 0.4942(4) | 0.8744(4) | 0.0338(6) |
| C7 | 0.46864(17) | 0.3553(3) | 0.7881(3) | 0.0336(6) |

**Table 4**. Bond lengths (Å) for **4**.

| | | | |
|---|---|---|---|
| Br1-C3 | 1.911(3) | C1-C6 | 1.364(5) |
| C1-C2 | 1.397(4) | C1-H1 | 0.95 |
| C2-C3 | 1.381(4) | C2-H4 | 0.95 |
| C3-C4 | 1.417(3) | C4-C5 | 1.430(4) |
| C4-C4 | 1.453(5) | C5-C6 | 1.404(4) |
| C5-C7 | 1.443(4) | C6-H2 | 0.95 |
| C7-C7 | 1.344(6) | C7-H3 | 0.95 |

**Table 5**. Bond angles (°) for **4**.

| | | | |
|---|---|---|---|
| C6-C1-C2 | 119.6(3) | C6-C1-H1 | 120.2 |
| C2-C1-H1 | 120.2 | C3-C2-C1 | 120.0(3) |
| C3-C2-H4 | 120.0 | C1-C2-H4 | 120.0 |
| C2-C3-C4 | 122.3(2) | C2-C3-Br1 | 114.76(19) |
| C4-C3-Br1 | 121.76(18) | C3-C4-C5 | 115.1(2) |
| C3-C4-C4 | 126.75(16) | C5-C4-C4 | 117.98(16) |
| C6-C5-C4 | 120.7(3) | C6-C5-C7 | 119.8(3) |
| C4-C5-C7 | 119.2(2) | C1-C6-C5 | 120.9(3) |
| C1-C6-H2 | 119.5 | C5-C6-H2 | 119.5 |
| C7-C7-C5 | 120.90(16) | C7-C7-H3 | 119.5 |
| C5-C7-H3 | 119.6 | | |

**Table 6**. Torsion angles (°) for **4.**

| | | | |
|---|---|---|---|
| C6-C1-C2-C3 | -5.9(4) | C1-C2-C3-C4 | -3.3(4) |
| C1-C2-C3-Br1 | 164.5(2) | C2-C3-C4-C5 | 12.3(3) |
| Br1-C3-C4-C5 | -154.62(18) | C2-C3-C4-C4 | -172.7(3) |
| Br1-C3-C4-C4 | 20.3(4) | C3-C4-C5-C6 | -12.9(3) |
| C4-C4-C5-C6 | 171.7(3) | C3-C4-C5-C7 | 161.3(2) |
| C4-C4-C5-C7 | -14.2(4) | C2-C1-C6-C5 | 5.2(4) |
| C4-C5-C6-C1 | 4.6(4) | C7-C5-C6-C1 | -169.5(2) |
| C6-C5-C7-C7 | 171.3(3) | C4-C5-C7-C7 | -2.8(4) |

**Table 7.** Anisotropic atomic displacement parameters ($Å^2$) for **4.**

The anisotropic atomic displacement factor exponent takes the form: $-2\pi^2[ h^2 a^{*2} U_{11} + ... + 2 h k a^* b^* U_{12} ]$

| | $U_{11}$ | $U_{22}$ | $U_{33}$ | $U_{23}$ | $U_{13}$ | $U_{12}$ |
|---|---|---|---|---|---|---|
| Br1 | 0.03698(19) | 0.02313(17) | 0.03713(19) | 0.00530(10) | 0.01051(12) | 0.00638(10) |
| C1 | 0.0276(14) | 0.0502(18) | 0.0370(15) | -0.0020(13) | 0.0117(11) | -0.0097(13) |
| C2 | 0.0275(13) | 0.0355(15) | 0.0337(14) | -0.0023(11) | 0.0064(10) | 0.0010(11) |
| C3 | 0.0285(12) | 0.0215(12) | 0.0255(12) | -0.0008(9) | 0.0048(9) | -0.0016(10) |
| C4 | 0.0269(12) | 0.0209(12) | 0.0215(11) | -0.0014(9) | 0.0016(9) | -0.0014(9) |
| C5 | 0.0306(13) | 0.0237(12) | 0.0237(12) | 0.0019(10) | -0.0016(10) | -0.0038(10) |
| C6 | 0.0352(15) | 0.0333(15) | 0.0310(14) | 0.0039(12) | 0.0043(11) | -0.0113(12) |
| C7 | 0.0460(16) | 0.0187(13) | 0.0318(14) | 0.0021(10) | 0.0010(11) | -0.0040(11) |

**Table 8**. Hydrogen atomic coordinates and isotropic atomic displacement parameters ($Å^2$) for **4**.

| | x/a | y/b | z/c | U(eq) |
|---|---|---|---|---|
| H1 | 0.2653 | 0.6229 | 0.9244 | 0.045 |
| H4 | 0.2990 | 0.8518 | 0.7978 | 0.039 |
| H2 | 0.3396 | 0.3987 | 0.9131 | 0.041 |
| H3 | 0.4501 | 0.2596 | 0.8240 | 0.04 |

GC/MS spectrum for 4-bromo-5-*tert*-butylphenanthrene **(5)**

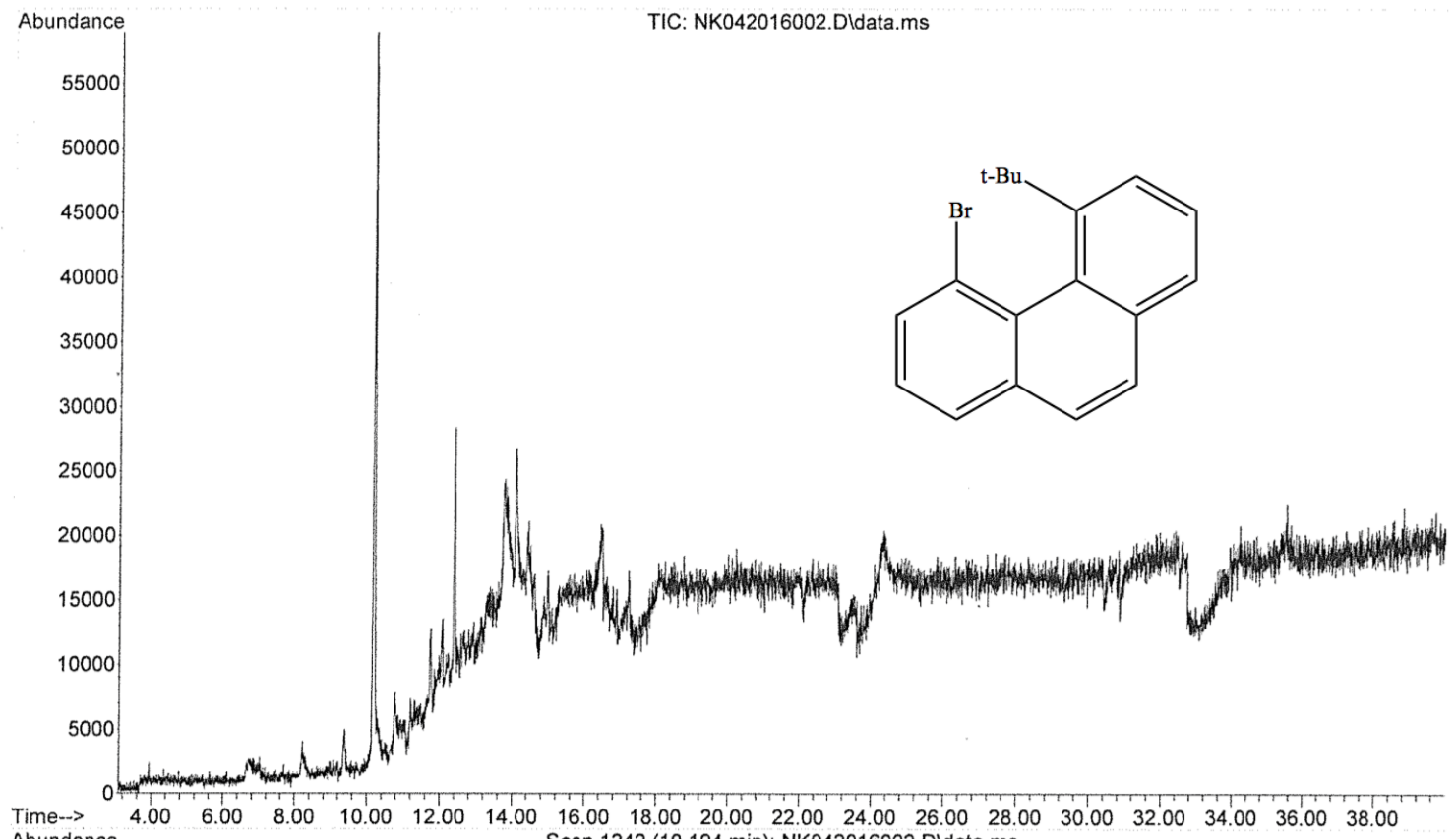


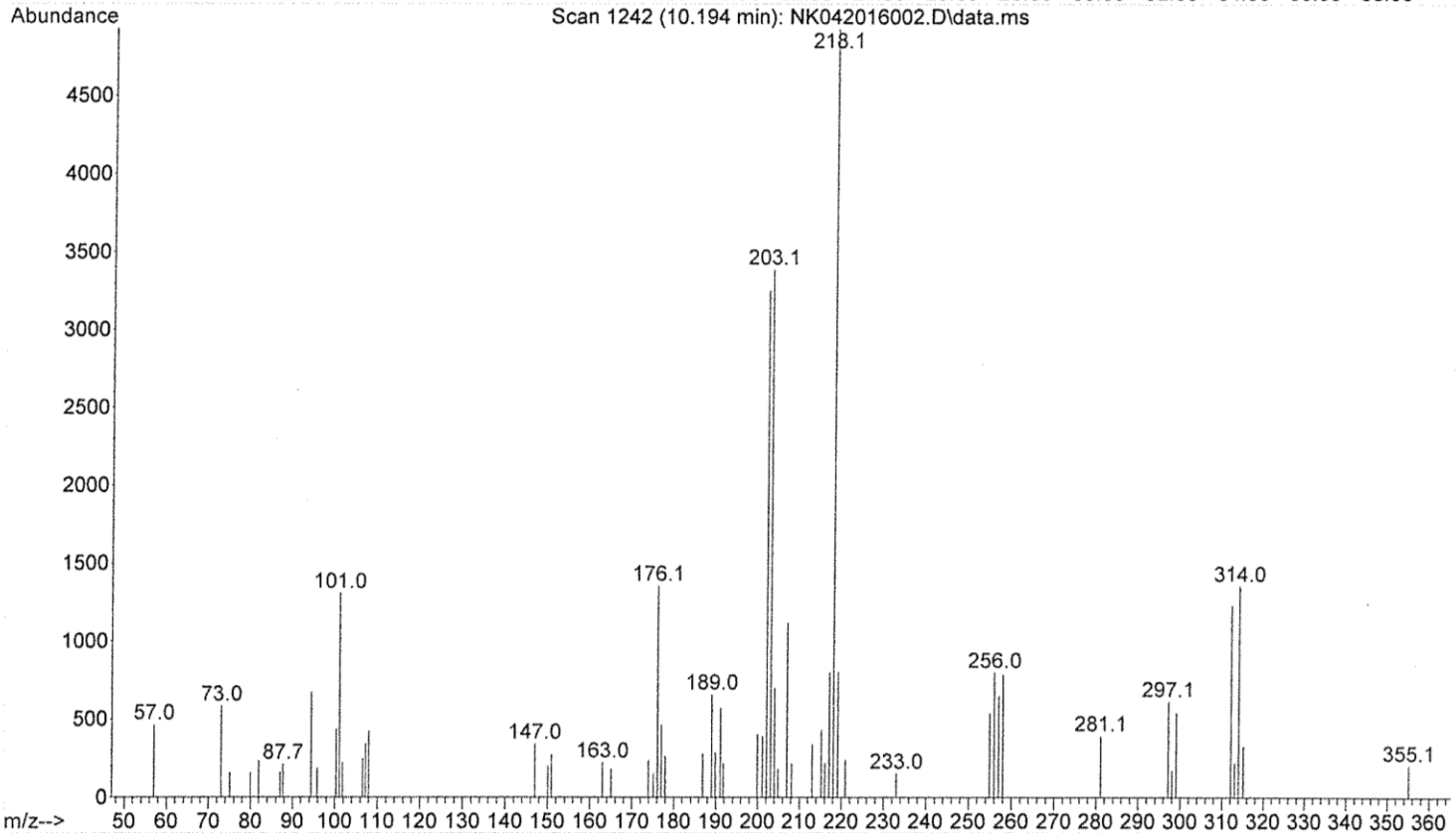

# Appendix B: Computational Results

## Gaussian Optimization Structures and Outputs



## Transition State Structure and Output

2,4-dimethyl-5,7-diphenylphenanthrene (**6**):

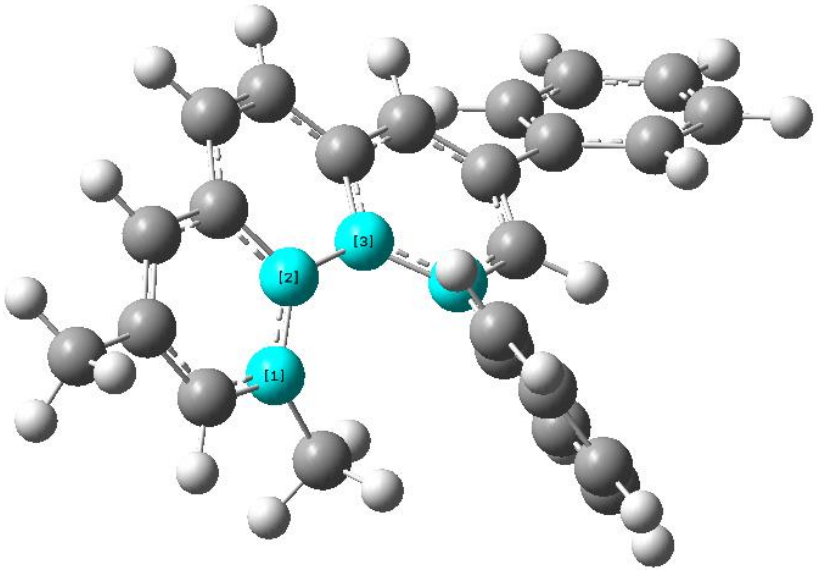


| | |
|---|---|
| Zero-point correction= | 0.303588 (Hartree/Particle) |
| Thermal correction to Energy= | 0.319127 |
| Thermal correction to Enthalpy= | 0.320071 |
| Thermal correction to Gibbs Free Energy= | 0.261396 |
| Sum of electronic and zero-point Energies= | -809.582220 |
| Sum of electronic and thermal Energies= | -809.566681 |
| Sum of electronic and thermal Enthalpies= | -809.565737 |
| Sum of electronic and thermal Free Energies= | -809.624412 |

Output Orientation

| Center Number | Atomic Number | Atomic Type | Coordinates (Angstroms) X | Y | Z |
|---|---|---|---|---|---|
| 1 | 6 | 0 | -5.712657 | -3.421982 | 0.096886 |
| 2 | 6 | 0 | -4.389959 | -3.357136 | -0.290949 |
| 3 | 6 | 0 | -3.806610 | -2.124085 | -0.652624 |
| 4 | 6 | 0 | -4.599062 | -0.931638 | -0.712628 |
| 5 | 6 | 0 | -5.902931 | -0.988272 | -0.114420 |
| 6 | 6 | 0 | -6.437366 | -2.231767 | 0.234837 |
| 7 | 6 | 0 | -2.388300 | -2.053471 | -0.867580 |
| 8 | 6 | 0 | -3.987653 | 0.259989 | -1.318006 |
| 9 | 6 | 0 | -2.554717 | 0.318497 | -1.358936 |
| 10 | 6 | 0 | -1.780995 | -0.863198 | -1.099485 |
| 11 | 6 | 0 | -1.894855 | 1.497581 | -1.764043 |
| 12 | 1 | 0 | -0.807890 | 1.520195 | -1.746749 |
| 13 | 6 | 0 | -2.617493 | 2.580782 | -2.221622 |
| 14 | 6 | 0 | -4.005198 | 2.456282 | -2.366051 |
| 15 | 6 | 0 | -4.702301 | 1.319147 | -1.961320 |
| 16 | 1 | 0 | -1.807742 | -2.967200 | -0.767396 |
| 17 | 1 | 0 | -6.164450 | -4.370073 | 0.375165 |
| 18 | 1 | 0 | -3.767688 | -4.248783 | -0.294219 |
| 19 | 1 | 0 | -7.417695 | -2.261894 | 0.700888 |
| 20 | 1 | 0 | -0.698573 | -0.794906 | -1.176133 |
| 21 | 1 | 0 | -2.114574 | 3.490888 | -2.537222 |
| 22 | 1 | 0 | -4.560697 | 3.255725 | -2.851558 |
| 23 | 6 | 0 | -6.661194 | 0.206532 | 0.359541 |
| 24 | 6 | 0 | -8.058349 | 0.280168 | 0.224868 |
| 25 | 6 | 0 | -6.009752 | 1.237959 | 1.056668 |
| 26 | 6 | 0 | -8.777855 | 1.350669 | 0.754339 |
| 27 | 1 | 0 | -8.581556 | -0.499087 | -0.323054 |
| 28 | 6 | 0 | -6.728188 | 2.309374 | 1.585544 |
| 29 | 1 | 0 | -4.933985 | 1.192393 | 1.192681 |
| 30 | 6 | 0 | -8.115095 | 2.373239 | 1.435635 |
| 31 | 1 | 0 | -9.856836 | 1.388347 | 0.627967 |
| 32 | 1 | 0 | -6.201906 | 3.093121 | 2.124276 |
| 33 | 1 | 0 | -8.673528 | 3.209323 | 1.847971 |
| 34 | 6 | 0 | -6.155340 | 1.234464 | -2.381221 |
| 35 | 1 | 0 | -6.822627 | 1.790899 | -1.716685 |
| 36 | 1 | 0 | -6.259881 | 1.662653 | -3.384672 |
| 37 | 1 | 0 | -6.512425 | 0.203132 | -2.420651 |

4,5-dibromophenanthrene **(4)**:

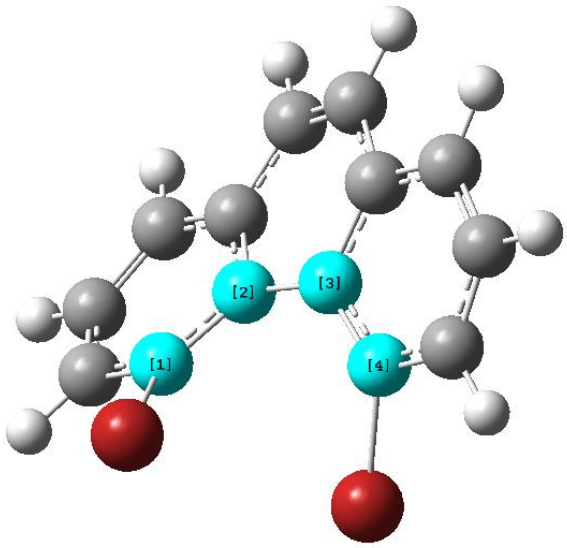


Output Orientation

| Center Number | Atomic Number | Atomic Type | Coordinates (Angstroms) X | Y | Z |
|---|---|---|---|---|---|
| 1 | 6 | 0 | -4.867020 | -3.134556 | 0.180456 |
| 2 | 6 | 0 | -3.496810 | -3.080100 | 0.347322 |
| 3 | 6 | 0 | -2.799727 | -1.863894 | 0.189273 |
| 4 | 6 | 0 | -3.510996 | -0.642590 | -0.045716 |
| 5 | 6 | 0 | -4.876677 | -0.789361 | -0.408283 |
| 6 | 6 | 0 | -5.550392 | -1.992210 | -0.260039 |
| 7 | 6 | 0 | -1.363100 | -1.861675 | 0.134474 |
| 8 | 6 | 0 | -2.754251 | 0.605910 | 0.001015 |
| 9 | 6 | 0 | -1.343027 | 0.540797 | -0.237646 |
| 10 | 6 | 0 | -0.680103 | -0.733865 | -0.186014 |
| 11 | 6 | 0 | -0.587832 | 1.721697 | -0.396375 |
| 12 | 1 | 0 | 0.472721 | 1.636273 | -0.617729 |
| 13 | 6 | 0 | -1.173245 | 2.961425 | -0.226986 |
| 14 | 6 | 0 | -2.501038 | 3.038161 | 0.216917 |
| 15 | 6 | 0 | -3.255149 | 1.884112 | 0.366160 |
| 16 | 1 | 0 | -0.844667 | -2.807073 | 0.271228 |
| 17 | 1 | 0 | -5.405579 | -4.069234 | 0.306533 |
| 18 | 1 | 0 | -2.929878 | -3.981128 | 0.565967 |
| 19 | 1 | 0 | -6.595783 | -2.051469 | -0.541265 |
| 20 | 1 | 0 | 0.397561 | -0.755794 | -0.325357 |
| 21 | 1 | 0 | -0.594248 | 3.871507 | -0.353796 |
| 22 | 1 | 0 | -2.931596 | 3.992055 | 0.500016 |
| 23 | 35 | 0 | -5.815871 | 0.555553 | -1.401358 |
| 24 | 35 | 0 | -4.879376 | 2.093652 | 1.364007 |

| | |
|---|---|
| Zero-point correction= | 0.173861 (Hartree/Particle) |
| Thermal correction to Energy= | 0.186284 |
| Thermal correction to Enthalpy= | 0.187228 |
| Thermal correction to Gibbs Free Energy= | 0.133705 |
| Sum of electronic and zero-point Energies= | -5681.546017 |
| Sum of electronic and thermal Energies= | -5681.533594 |
| Sum of electronic and thermal Enthalpies= | -5681.532650 |
| Sum of electronic and thermal Free Energies= | -5681.586172 |

---

4-bromo-5-*tert*-butylphenanthrene **(5b)**:

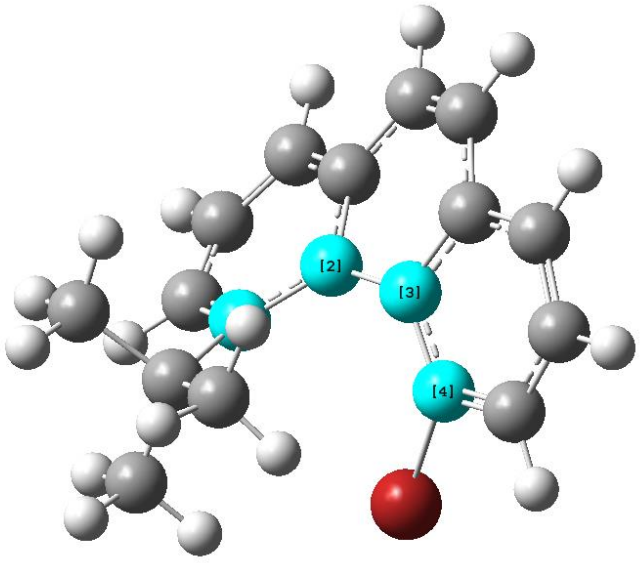


| | |
|---|---|
| Zero-point correction= | 0.297353 (Hartree/Particle) |
| Thermal correction to Energy= | 0.313610 |
| Thermal correction to Enthalpy= | 0.314554 |
| Thermal correction to Gibbs Free Energy= | 0.254750 |
| Sum of electronic and zero-point Energies= | -3267.557416 |
| Sum of electronic and thermal Energies= | -3267.541159 |
| Sum of electronic and thermal Enthalpies= | -3267.540214 |
| Sum of electronic and thermal Free Energies= | -3267.600019 |

Output Orientation

| Center Number | Atomic Number | Atomic Type | Coordinates (Angstroms) X | Y | Z |
|---|---|---|---|---|---|
| 1 | 6 | 0 | -5.644491 | -4.593397 | -1.265679 |
| 2 | 6 | 0 | -4.369512 | -4.649807 | -0.741183 |
| 3 | 6 | 0 | -3.776606 | -3.481253 | -0.224393 |
| 4 | 6 | 0 | -4.461323 | -2.222706 | -0.299992 |
| 5 | 6 | 0 | -5.879005 | -2.248833 | -0.538113 |
| 6 | 6 | 0 | -6.394402 | -3.421828 | -1.099986 |
| 7 | 6 | 0 | -2.516992 | -3.566122 | 0.465986 |
| 8 | 6 | 0 | -3.615269 | -1.039173 | -0.112129 |
| 9 | 6 | 0 | -2.426953 | -1.158208 | 0.681516 |
| 10 | 6 | 0 | -1.936839 | -2.468022 | 1.012147 |
| 11 | 6 | 0 | -1.658818 | -0.018102 | 1.000689 |
| 12 | 1 | 0 | -0.792882 | -0.139223 | 1.646445 |
| 13 | 6 | 0 | -1.957524 | 1.214097 | 0.451974 |
| 14 | 6 | 0 | -2.981079 | 1.307738 | -0.501981 |
| 15 | 6 | 0 | -3.761680 | 0.198533 | -0.786688 |
| 16 | 1 | 0 | -2.073231 | -4.550645 | 0.592013 |
| 17 | 1 | 0 | -6.103553 | -5.472003 | -1.710606 |
| 18 | 1 | 0 | -3.814148 | -5.583707 | -0.708386 |
| 19 | 1 | 0 | -7.450179 | -3.463543 | -1.347220 |
| 20 | 1 | 0 | -1.028181 | -2.546683 | 1.603213 |
| 21 | 1 | 0 | -1.360431 | 2.089367 | 0.690843 |
| 22 | 1 | 0 | -3.144263 | 2.229869 | -1.048264 |
| 23 | 6 | 0 | -6.954376 | -1.278806 | 0.060342 |
| 24 | 6 | 0 | -7.679865 | -2.111145 | 1.159985 |
| 25 | 1 | 0 | -8.164550 | -3.002748 | 0.752167 |
| 26 | 1 | 0 | -6.974161 | -2.437655 | 1.932404 |
| 27 | 1 | 0 | -8.450899 | -1.497625 | 1.641680 |
| 28 | 6 | 0 | -6.431612 | -0.020299 | 0.783480 |
| 29 | 1 | 0 | -5.661077 | -0.261493 | 1.522012 |
| 30 | 1 | 0 | -6.037000 | 0.728196 | 0.098327 |
| 31 | 1 | 0 | -7.268924 | 0.440436 | 1.320569 |
| 32 | 6 | 0 | -8.004369 | -0.839824 | -0.986151 |
| 33 | 1 | 0 | -8.767320 | -0.218228 | -0.502303 |
| 34 | 1 | 0 | -7.543546 | -0.253269 | -1.783382 |
| 35 | 1 | 0 | -8.521969 | -1.689743 | -1.442257 |
| 36 | 35 | 0 | -4.911600 | 0.371391 | -2.317228 |

4,5-bis-*tert*-butylphenanthrene **(5)**:

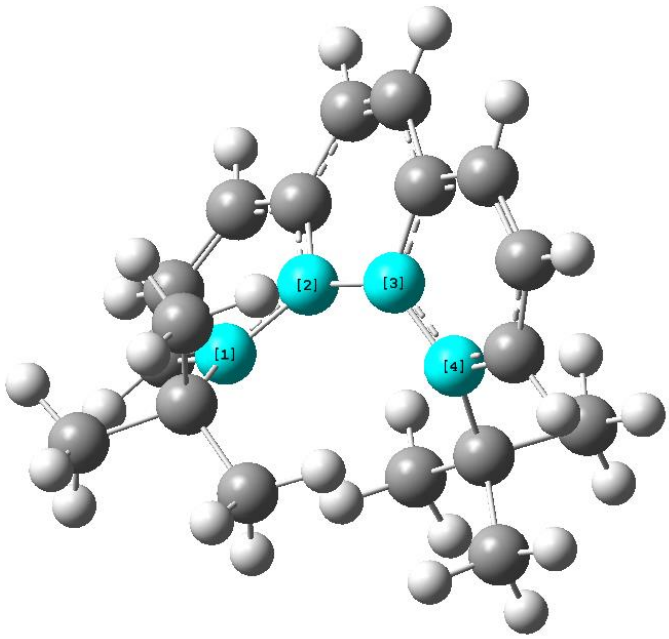


| | |
|---|---|
| Zero-point correction= | 0.420616 (Hartree/Particle) |
| Thermal correction to Energy= | 0.440784 |
| Thermal correction to Enthalpy= | 0.441728 |
| Thermal correction to Gibbs Free Energy= | 0.374742 |
| Sum of electronic and zero-point Energies= | -853.555196 |
| Sum of electronic and thermal Energies= | -853.535029 |
| Sum of electronic and thermal Enthalpies= | -853.534084 |
| Sum of electronic and thermal Free Energies= | -853.601071 |

Output Orientation

| Center Number | Atomic Number | Atomic Type | Coordinates (Angstroms) X | Y | Z |
|---|---|---|---|---|---|
| 1 | 6 | 0 | -6.248218 | -4.791512 | 0.002559 |
| 2 | 6 | 0 | -4.886877 | -4.832204 | 0.232556 |
| 3 | 6 | 0 | -4.121942 | -3.655212 | 0.109453 |
| 4 | 6 | 0 | -4.766252 | -2.396098 | -0.133814 |
| 5 | 6 | 0 | -6.084515 | -2.439352 | -0.710021 |
| 6 | 6 | 0 | -6.807852 | -3.626306 | -0.540069 |
| 7 | 6 | 0 | -2.684014 | -3.721866 | 0.085709 |
| 8 | 6 | 0 | -3.955554 | -1.197567 | 0.135812 |
| 9 | 6 | 0 | -2.557570 | -1.310110 | -0.152036 |
| 10 | 6 | 0 | -1.951379 | -2.615380 | -0.199752 |
| 11 | 6 | 0 | -1.754885 | -0.153557 | -0.240138 |
| 12 | 1 | 0 | -0.709234 | -0.255245 | -0.520534 |
| 13 | 6 | 0 | -2.294469 | 1.075802 | 0.074149 |
| 14 | 6 | 0 | -3.570445 | 1.128586 | 0.658882 |
| 15 | 6 | 0 | -4.399508 | 0.011187 | 0.786107 |
| 16 | 1 | 0 | -2.213384 | -4.695915 | 0.194191 |
| 17 | 1 | 0 | -6.860254 | -5.681142 | 0.124329 |
| 18 | 1 | 0 | -4.385417 | -5.765936 | 0.475172 |
| 19 | 1 | 0 | -7.821171 | -3.688365 | -0.922603 |
| 20 | 1 | 0 | -0.876754 | -2.676881 | -0.352987 |
| 21 | 1 | 0 | -1.703515 | 1.983400 | -0.014667 |
| 22 | 1 | 0 | -3.882316 | 2.076125 | 1.079807 |
| 23 | 6 | 0 | -5.533578 | 0.049628 | 1.866558 |
| 24 | 6 | 0 | -5.443441 | 1.337504 | 2.720213 |
| 25 | 1 | 0 | -4.454801 | 1.468116 | 3.172330 |
| 26 | 1 | 0 | -5.683199 | 2.238585 | 2.144016 |
| 27 | 1 | 0 | -6.174917 | 1.272515 | 3.533214 |
| 28 | 6 | 0 | -6.602773 | -1.483990 | -1.840023 |
| 29 | 6 | 0 | -8.125556 | -1.217670 | -1.779171 |
| 30 | 1 | 0 | -8.419220 | -0.620191 | -2.650189 |
| 31 | 1 | 0 | -8.719030 | -2.136182 | -1.812510 |
| 32 | 1 | 0 | -8.414498 | -0.660498 | -0.884803 |
| 33 | 6 | 0 | -5.887863 | -0.127773 | -1.986876 |
| 34 | 1 | 0 | -6.045272 | 0.533683 | -1.135159 |
| 35 | 1 | 0 | -4.809932 | -0.243852 | -2.124893 |
| 36 | 1 | 0 | -6.283023 | 0.376981 | -2.876932 |
| 37 | 6 | 0 | -6.315474 | -2.262690 | -3.158763 |
| 38 | 1 | 0 | -6.855026 | -3.214357 | -3.190837 |
| 39 | 1 | 0 | -6.625157 | -1.663505 | -4.024187 |
| 40 | 1 | 0 | -5.246292 | -2.479259 | -3.259448 |
| 41 | 6 | 0 | -5.301970 | -1.138426 | 2.836748 |
| 42 | 1 | 0 | -4.290539 | -1.109793 | 3.257626 |
| 43 | 1 | 0 | -6.016833 | -1.083384 | 3.666935 |
| 44 | 1 | 0 | -5.435602 | -2.104054 | 2.343419 |
| 45 | 6 | 0 | -6.983139 | -0.022061 | 1.349563 |
| 46 | 1 | 0 | -7.213862 | 0.808297 | 0.673653 |
| 47 | 1 | 0 | -7.182528 | -0.961709 | 0.836793 |
| 48 | 1 | 0 | -7.675037 | 0.044211 | 2.198568 |

Transition State of 4,5-dibromophenanthrene **(4)**:

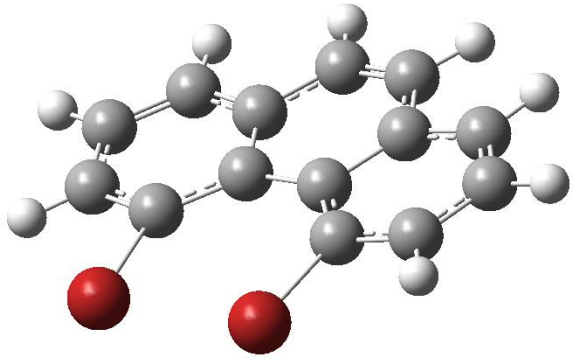

| | |
|---|---|
| Zero-point correction= | 0.174094 (Hartree/Particle) |
| Thermal correction to Energy= | 0.185841 |
| Thermal correction to Enthalpy= | 0.186785 |
| Thermal correction to Gibbs Free Energy= | 0.133371 |
| Sum of electronic and zero-point Energies= | -5681.512880 |
| Sum of electronic and thermal Energies= | -5681.501132 |
| Sum of electronic and thermal Enthalpies= | -5681.500188 |
| Sum of electronic and thermal Free Energies= | -5681.553602 |

Output Orientation

| Center Number | Atomic Number | Atomic Type | Coordinates (Angstroms) X | Y | Z |
|---|---|---|---|---|---|
| 1 | 6 | 0 | -3.596356 | 1.164715 | 0.751798 |
| 2 | 6 | 0 | -2.746274 | 2.219854 | 0.557999 |
| 3 | 6 | 0 | -1.382476 | 2.022602 | 0.250950 |
| 4 | 6 | 0 | -0.751594 | 0.714999 | 0.106643 |
| 5 | 6 | 0 | -1.720339 | -0.343751 | 0.291267 |
| 6 | 6 | 0 | -3.060455 | -0.109451 | 0.608650 |
| 7 | 6 | 0 | -0.668935 | 3.250343 | 0.098118 |
| 8 | 6 | 0 | 0.739019 | 0.718321 | -0.179304 |
| 9 | 6 | 0 | 1.372876 | 2.028746 | -0.277651 |
| 10 | 6 | 0 | 0.648160 | 3.253281 | -0.154575 |
| 11 | 6 | 0 | 2.752622 | 2.232127 | -0.496902 |
| 12 | 1 | 0 | 3.109217 | 3.256382 | -0.549392 |
| 13 | 6 | 0 | 3.618612 | 1.180817 | -0.632272 |
| 14 | 6 | 0 | 3.073270 | -0.095761 | -0.568020 |
| 15 | 6 | 0 | 1.711866 | -0.336099 | -0.367117 |
| 16 | 1 | 0 | -1.222821 | 4.178389 | 0.202266 |
| 17 | 1 | 0 | -4.644830 | 1.301796 | 0.997376 |
| 18 | 1 | 0 | -3.101375 | 3.242518 | 0.642110 |
| 19 | 1 | 0 | -3.705258 | -0.968482 | 0.738397 |
| 20 | 1 | 0 | 1.197255 | 4.183783 | -0.262114 |
| 21 | 1 | 0 | 4.682927 | 1.322613 | -0.792031 |
| 22 | 1 | 0 | 3.724003 | -0.951899 | -0.686824 |
| 23 | 35 | 0 | -1.545753 | -2.261985 | 0.152849 |
| 24 | 35 | 0 | 1.506710 | -2.255178 | -0.432801 |